Astro Dark (Says it All)

-

Cosmo, PP, QG, BH theory…

Lisa Randall AstroDark 2021

What is a keynote?
Where are we?

- SM understood
- DM understood
  - Many consistent measurements
    - A few less consistent
  - But what is it?
  - And how will we ever know
- GW measurements understood in part
  - What will we learn from them
- Light particles not yet really understood
  - Also we are not sure if we are missing some
  - More appreciation of "hiding in plain sight"
    - Where "sight" is a very subtle technique for finding things that don't interact much

Where to Focus?

- Dark Matter
- Light Matter
  - Axions
  - Neutrinos
- Primordial Black Holes
- Gravity Waves
  - Standard astro
  - BSM

Where else to focus?

- Also
- Questions about inflation
  - How does it start and how does it end
- Questions about phase transitions
  - Can RS complete
  - Are there first order transitions
- Interesting interface our methods/studies and formal work
  - KKLT: String theory vacua
    - Focus on potential instability and correct EFT
  - Entanglement entropy, information transfer
    - Focus on using KR as a model
    - Rich environment to ask tractable questions

I: Dark Matter

- Before “alternative theories of dark matter”
- Now recognition there is no standard bearer
- Need to think creatively of how to search
  - And to define limits of what we are really searching for
  - And how reliable our results are
- Many models now at this conference and elsewhere

My keynote; one of my dark matter models

- DDDM
  - Doesn't say what majority of dark matter is
  - But allows an additional dissipative component
    - Simplest example is dark matter carrying its own (dark) charge
  - Consequence might be dissipation and a dark disk
  - Many potential observational implications
  - Most direct way to bound DDDM
    - Use kinematics
    - Several papers did that

Results

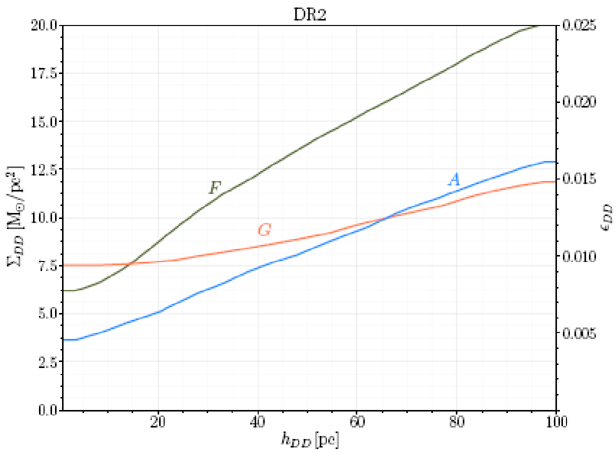

Figure 7: 95% CR upper limit contours for surface density Σ_{DD} and scale height h_{DD} of a thin DD for A (blue), F(green), and G (orange) stars using data from DR2 (left panel) and TGAS (right). The upper bound for the fraction of the total DM mass in the MW that could exist in a DD, ϵ_{DD}, is also shown on the right side of each plot for reference.

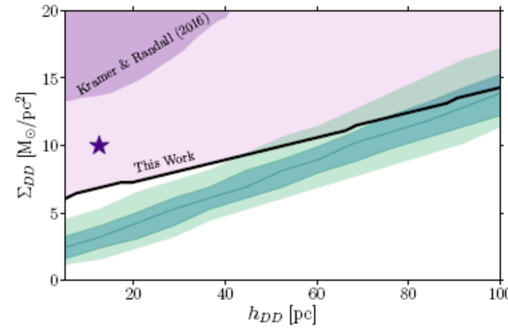

FIG. 2. The 95% constraint on the DD surface density Σ_{DD} as a function of the scale height h_{DD}, as found in this work and in Ref. [51] (Kramer & Randall 2016). The star indicates fiducial DD parameters that can account for phenomena such as periodic comet impacts [36]. Also shown is a comparison of the limit to the 68% and 95% containment regions (in dark and light green, respectively) on the expected limit from simulated data generated under the null hypothesis of no DD.

Buch, Chau, Fan

Stellar type	$\rho_{\rm DM}$ [$M_\odot/\mathrm{pc}^3$]	$\rho_{\rm DM}$ [GeV/cm^3]	ρ_b [$M_\odot/\mathrm{pc}^3$]	$z_\odot$ [pc]
A stars	$0.016^{+0.010}_{-0.010}$	$0.608^{+0.380}_{-0.380}$	$0.088^{+0.007}_{-0.007}$	$8.80^{+3.74}_{-4.23}$
F stars	$0.039^{+0.008}_{-0.008}$	$1.482^{+0.304}_{-0.304}$	$0.089^{+0.007}_{-0.007}$	$2.04^{+2.84}_{-3.13}$
G stars	$0.011^{+0.010}_{-0.009}$	$0.418^{+0.380}_{-0.342}$	$0.087^{+0.007}_{-0.007}$	$-8.82^{+5.32}_{-4.64}$

(Schutz et al: -1.3 ± 4.6 pc)

Table 5: Median posterior values with 1σ errors for the local densities of baryons ρ_b and halo DM $\rho_{\rm DM}$, and height of the sun above the midplane $z_\odot$. The halo DM density $\rho_{\rm DM}$ is expressed in both $M_\odot/\mathrm{pc}^3$ (astronomical unit) and GeV/cm^3 (particle physics unit), where $1\ M_\odot/\mathrm{pc}^3 \approx 38$ GeV/cm^3.

What really is ruled out?

- Each one has a different solar height
  - Implies systematic effects
  - Indicating dynamical system
  - So dark disk not ruled out
  - And actually hard to determine
    - Velocity dispersion sensitivity
    - Challenge to determine how to address this
- Don't know answer
  - No supporting evidence
  - But not ruled out
    - (Kind of like most models of dark matter…)
  - (Actually you can't rule it out—just bound it)

Measuring the local matter density using Gaia DR2
A. Widmark

- Excess surface density of approximately 5–9 Mpc⍰
- Mild tension with Schutz et al. (2018) and Buch et al. (2018), who report 95 % constraints of around 7 Mpc⍰ to a surplus matter density with a scale height of 30 pc.
- Older papers only use the velocity information of stars close to the Galactic plane, and have fewer and smaller stellar samples.

The results for the vertical velocity of the Sun with respect to the Galactic plane (4.76 ± 2.27 pc) agree well with Buch et al. (2018), but is in tension with e Juric et al. (2008); Yao et al. (2017); Widmark & Monari (2018); Bennett & Bovy (2019), who report higher values of 25 ± 5 pc, 13.4 ± 4.4 pc, 15.3 ± 2.2 pc, and 20.8 ± 0.3 pc, respectively. Bennett & Bovy (2019) demonstrate that the distribution of stars is not symmetric across the Galactic plane, and exhibit wave-like patterns in both number density and vertical velocity

. Mdzsurements of the Sun's position with respect to the mid-plane can differ depending on how the mid-plane is defined, and what distance cuts are made in the analysis. Juric et al. (2008); Yao et al. (2017); Bennett & Bovy (2019) all extend to kpc distances and fit symmetric stellar number density distributions, which could explain why they all infer higher values.

- Conclude it is difficult to constrain the density
- And we don't yet know how to improve it
- Need more data, better methods and models

II. Next AD topic: What can particle physicists say about gravity waves

- Perhaps not surprisingly small pickings
  - Gravity is a weak force so signal requires huge effects
  - Yet for big massive objects quadrupole often dominates over NP
    - Hard to collect enough new stuff to affect signal

- At least two very interesting arenas in NP
  - Axion like particles and superradiance
  - Phase transitions
  - More?

So far however: It’s measurements of GW binaries at LIGO that have been spectacularly successful

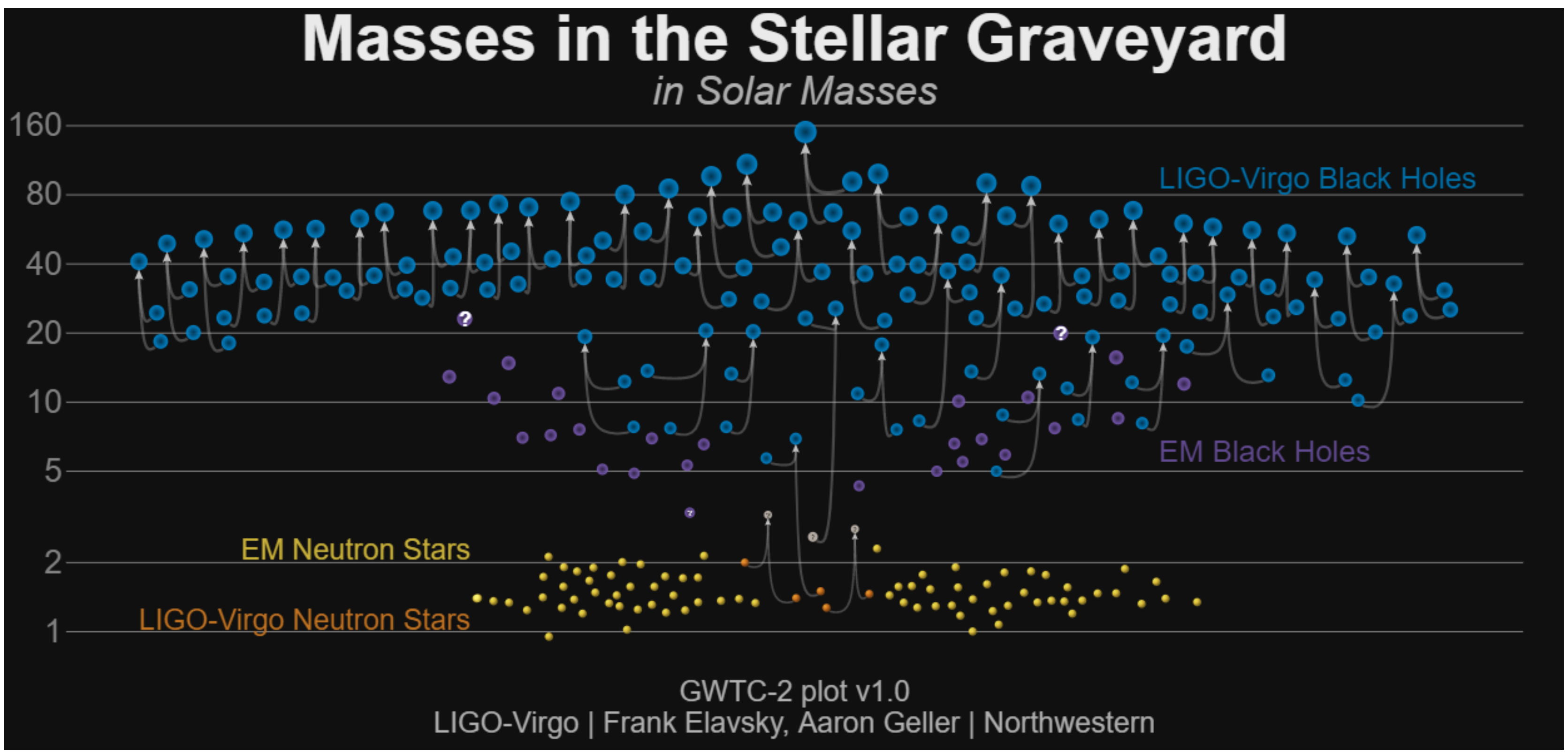

But sometimes new stuff in old arenas

- Zhong-Zhi Xianyu and I started investigating eccentricity as a way of distinguishing populations in
  - Was told hopeless since quadrupole kills eccentricity
  - And indeed LIGO has seen very little evidence of eccentric events
- But spin has not proved to be as powerful a distinguishing factor as had been hoped
- So now lots of attention to eccentricity

But…Spin not great discriminator either

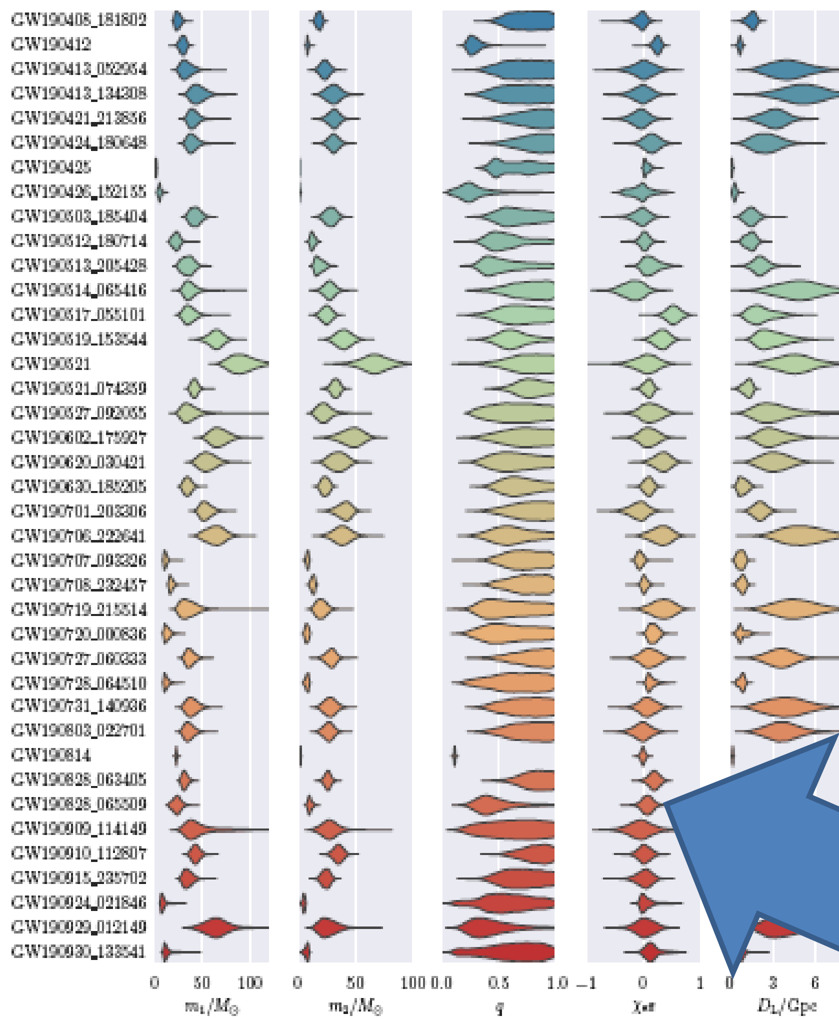

FIG. 8. Marginal posterior distributions on primary mass m_1, secondary mass m_2, mass ratio q, effective spin $\chi_{\rm eff}$, and the luminosity distance d_L for all candidate events in O3a. The vertical extent of each colored region is proportional to one-dimensional marginal posterior distribution at a given parameter value for the corresponding event.

Why is eccentricity interesting?

- Tells about formation channel
- Generally need some dynamical effect from something external to the black hole binary
  - Can be globular clusters
    - Can be perturbative
    - Or chaotic/multibody
  - Can be black hole at center of galaxy
  - Can be field triples
- How to tell them apart?

Several Dynamical Systems of Interest

SMBH in galactic center or IMBH in a globular cluster

Stellar mass inducing tidal force (with orbiting system)

BBH in stellar-mass hierarchical triples in globular clusters or in isolated galactic regions

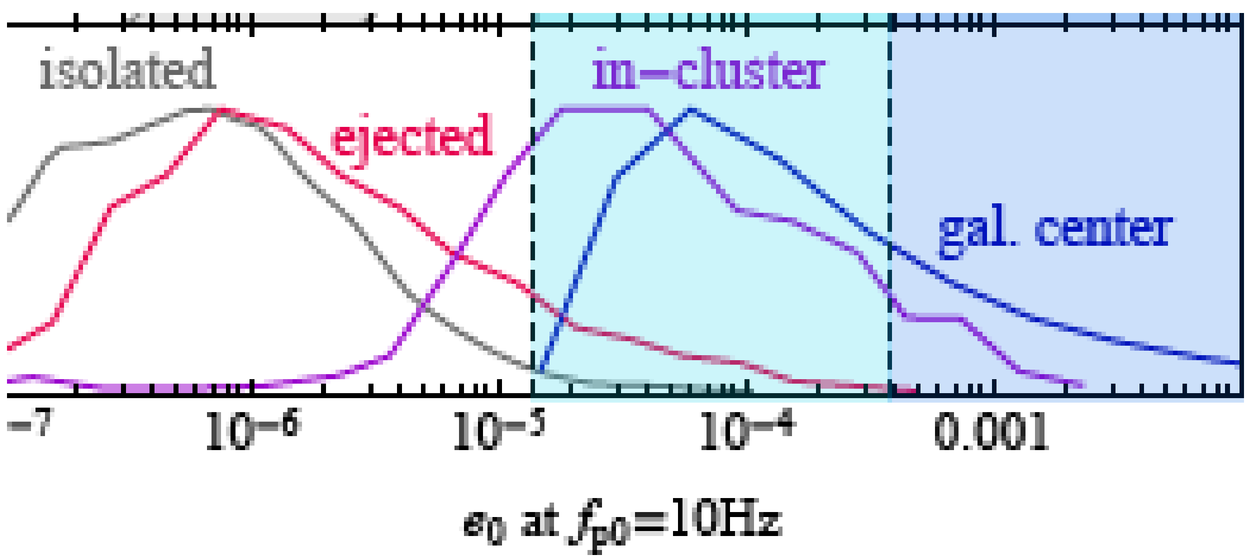

GW190521: 150 Solar Mass?

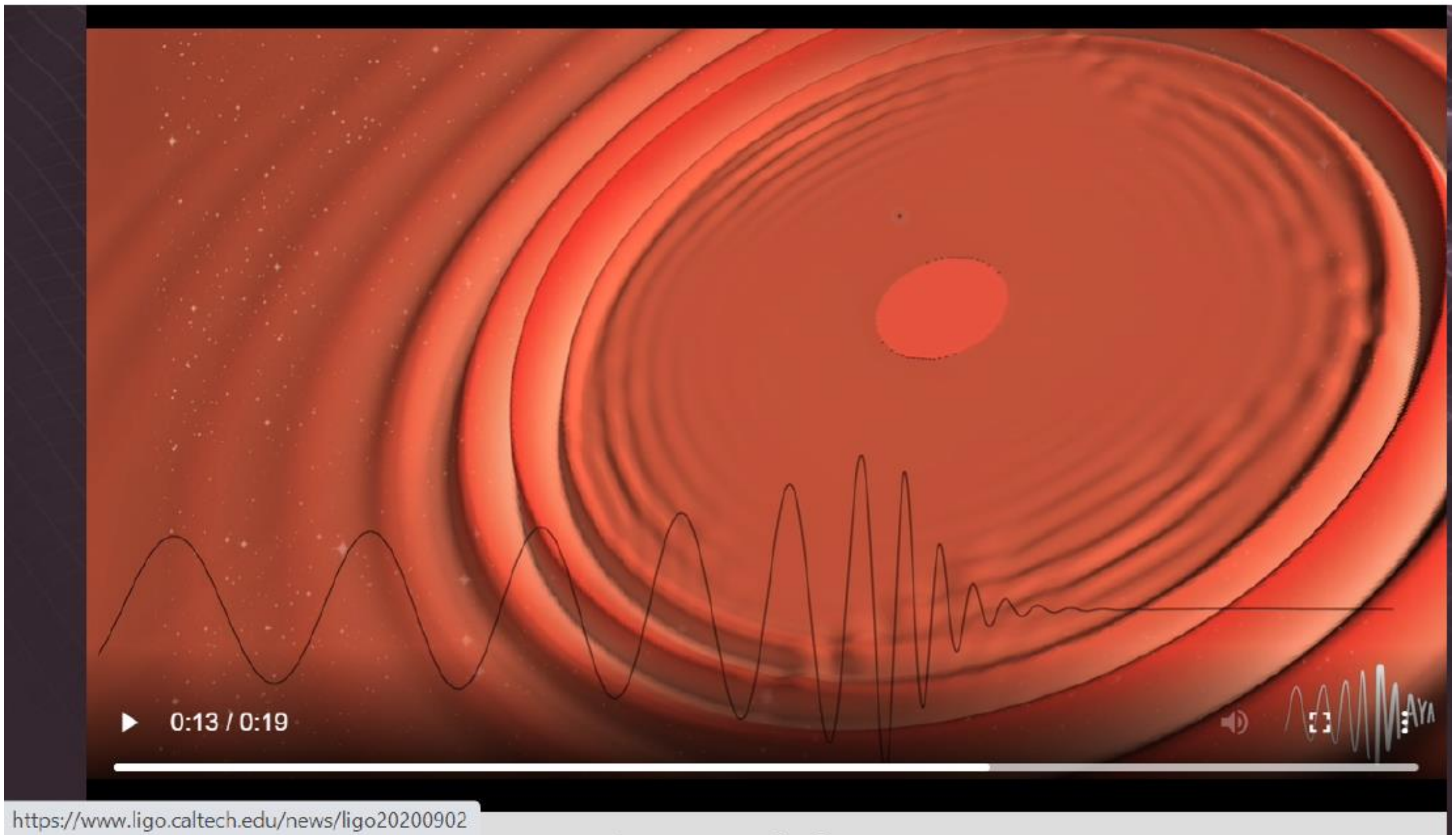

Evidence for Dynamical Formation: GW190521

GW190521 as a Highly Eccentric Black Hole Merger

V. Gayathri,[1] J. Healy,[2] J. Lange,[2] B. O'Brien,[1] M. Szczepańczyk,[1] I. Bartos,[1,*] M. Campanelli,[2] S. Klimenko,[1] C. Lousto,[2] and R. O'Shaughnessy[2,†]

Parameters	This work	LIGO/Virgo
Primary mass [$M_\odot$]	102^{+7}_{-11}	85^{+21}_{-14}
Secondary mass [$M_\odot$]	102^{+7}_{-11}	66^{+17}_{-18}
Total mass [$M_\odot$]	204^{+14}_{-33}	150^{+29}_{-17}
Mass ratio	1	$0.79^{+0.19}_{-0.29}$
Luminosity distance [Gpc]	$1.84^{+1.07}_{-0.054}$	$5.3^{+2.4}_{-2.6}$
Redshift	$0.35^{+0.16}_{-0.09}$	$0.82^{+0.28}_{-0.34}$
Eccentricity	0.67	0
Effective spin ($\chi_{\rm eff}$)	0	$0.08^{+0.27}_{-0.36}$
Precession spin ($\chi_{\rm p}$)	0.7	$0.68^{+0.25}_{-0.37}$

TABLE I. Reconstructed properties of GW190521 by this work. For comparison we also show the properties obtained by LIGO/Virgo [3, 4] using the NRSur7dq4 non-eccentric, precessing waveform model [50].

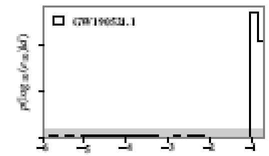

GW190521: ORBITAL ECCENTRICITY AND SIGNATURES OF DYNAMICAL FORMATION IN A BINARY BLACK HOLE MERGER SIGNAL

Isobel Romero-Shaw,[1,2] Paul D. Lasky,[1,2] Eric Thrane,[1,2] and Juan Calderón Bustillo[1,2,3]

Table 1. Recovered GW190521 parameter values IMRPHENOMPv2 and NRSUR7DQ4, and NRSUR7DQ4 constrained to have aligned spins. For the SEOBNRE analysis, we give the 90% confidence lower limit on eccentricity at 10 Hz. For other parameters, the median of the posterior is given along with the 90% credible interval. In the final column, we state the values inferred from the LIGO–Virgo analysis, read from the public posterior samples obtained using NRSUR7DQ4 (Abbott et al. 2020a). In the final row, we provide the log Bayes factor of each analysis against the signal-to-noise log Bayes factor obtained for $e_{10} \geq 0.1$ using SEOBNRE ($\ln \mathcal{B}_{S/N} = 85.7$).

Parameter (source frame)	SEOBNRE	IMRPHENOMPv2	NRSUR7DQ4	NRSUR7DQ4 aligned	NRSUR7DQ4 LVC
Primary mass, m_1 [$M_\odot$]	92^{+26}_{-16}	126^{+61}_{-41}	86^{+18}_{-13}	85^{+22}_{-14}	85^{+21}_{-14}
Secondary mass, m_2 [$M_\odot$]	69^{+18}_{-19}	59^{+32}_{-24}	69^{+18}_{-17}	61^{+15}_{-17}	66^{+17}_{-18}
Luminosity distance, $d_{\rm L}$ [Gpc]	$4.1^{+1.8}_{-1.8}$	$2.4^{+2.3}_{-1.0}$	$4.7^{+2.2}_{-2.2}$	$4.7^{+1.6}_{-1.5}$	$5.3^{+2.4}_{-2.6}$
Right ascension, α [rad]	$3.6^{+2.7}_{-3.5}$	$4.3^{+1.9}_{-4.3}$	$3.4^{+2.9}_{-3.4}$	$3.7^{+2.6}_{-3.7}$	$3.5^{+2.8}_{-3.4}$
Declination, δ [rad]	$-0.7^{+1.4}_{-0.5}$	$-0.7^{+1.5}_{-0.4}$	$-0.8^{+1.5}_{-0.4}$	$-0.9^{+1.6}_{-0.3}$	$-0.8^{+1.5}_{-0.4}$
Reference phase, ϕ [rad]	$3.1^{+2.9}_{-2.7}$	$3.0^{+3.0}_{-2.7}$	$3.2^{+2.6}_{-2.6}$	$3.1^{+2.9}_{-2.8}$	$3.4^{+2.6}_{-3.2}$
Polarisation, ψ [rad]	$1.5^{+1.5}_{-1.4}$	$1.6^{+1.3}_{-1.5}$	$1.8^{+1.2}_{-1.5}$	$1.6^{+1.4}_{-1.4}$	$1.8^{+1.2}_{-1.6}$
Inclination, $\theta_{\rm JN}$ [rad]	$1.3^{+1.6}_{-1.0}$	$1.4^{+1.0}_{-0.7}$	$0.8^{+2.0}_{-0.6}$	$0.7^{+2.2}_{-0.5}$	$0.8^{+2.1}_{-0.6}$
Eccentricity lower limit at 10 Hz, $e_{10}^{\rm min}$	0.11	N/A	N/A	N/A	N/A
Effective spin, $\chi_{\rm eff}$	$0.0^{+0.2}_{-0.2}$	$0.1^{+0.4}_{-0.4}$	$0.0^{+0.3}_{-0.3}$	$0.0^{+0.2}_{-0.3}$	$0.1^{+0.3}_{-0.4}$
Effective precession, χ_p	N/A	$0.7^{+0.2}_{-0.3}$	$0.6^{+0.2}_{-0.3}$	N/A	$0.7^{+0.3}_{-0.4}$
Log Bayes factor against SEOBNRE, $\ln \mathcal{B}_{X/E}$	0.0	−2.0	−1.8	−5.0	−1.2

ABSTRACT

Pair instability supernovae are thought to restrict the formation of black holes in the mass range ~ 50 – 135 $M_\odot$. However, black holes with masses within this "high mass gap" are expected to form as the remnants of binary black hole mergers. These remnants can merge again dynamically in densely populated environments such as globular clusters. The hypothesis that the binary black hole merger GW190521 formed dynamically is supported by its high mass. Orbital eccentricity can also be a signature of dynamical formation, since a binary that merges quickly after becoming bound may not circularize before merger. In this work, we measure the orbital eccentricity of GW190521. We find that the data prefer a signal with eccentricity $e \geq 0.1$ at 10 Hz to a non-precessing, quasi-circular signal, with a log Bayes factor $\ln \mathcal{B} = 5.0$. When compared to precessing, quasi-circular analyses, the data prefer a non-precessing, $e \geq 0.1$ signal, with log Bayes factors $\ln \mathcal{B} \approx 2$. Using injection studies, we find that a non-spinning, moderately eccentric ($e = 0.13$) GW190521-like binary can be mistaken for a quasi-circular, precessing binary. Conversely, a quasi-circular binary with spin-induced precession may be mistaken for an eccentric binary. We therefore cannot confidently determine whether GW190521 was precessing or eccentric. Nevertheless, since both of these properties support the dynamical formation hypothesis, our findings support the hypothesis that GW190521 formed dynamically.

Beyond aLIGO What can we learn from LISA (about formation channel)?

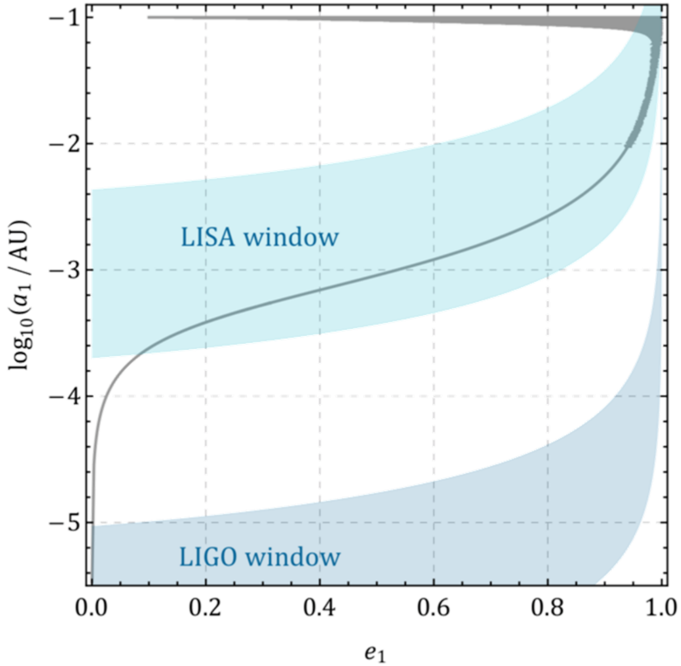

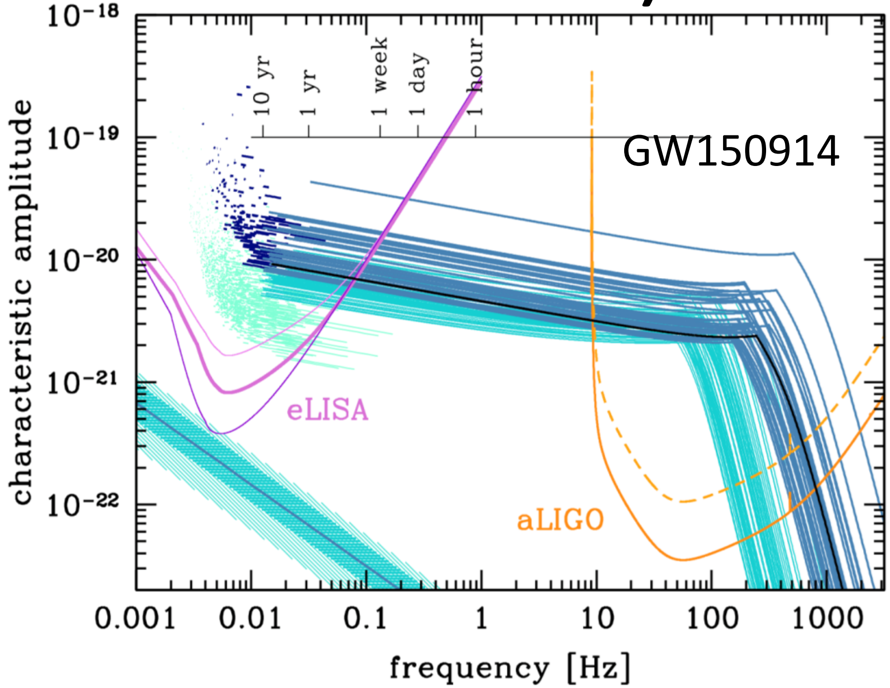

Sesana, 1602.06951

Environment: aLIGO vs LISA

- With aLIGO we have the potential to measure eccentricity statistically
  - LISA can do more complete *e* measurement: larger (hasn't yet been radiated away)
- We will also see we can learn about formation channel even without measuring carefully
- ALSO: with LISA we also have the potential to measure outer orbital motion **directly**

LISA Observations of Triples

- LISA observes events for ~[4]5 (10?) years
- Stellar mass binaries can be in LISA window
  – Even if not merging there
- Possible many stellar mass binaries in triple systems
  - Triple systems allow for generation of eccentricity, more likely to merge in short enough time
  – eg 1602.03831.pdf Bartos, Kocsis, Haiman, Marka argue significant fraction LIGO events can come from binary mergers in accretion disk
    - Migrate toward central black hole
  – 1608.07642.pdf Kedron Silsbee 1 & Scott Tremaine 2 argue KL plays a big role even for "isolated systems
  – For certain binary parameter ranges, can monitor time evolution
  – Can then study change in orbital parameters
- **Direct probe of dynamics and ambient density distribution**
  – **Directly measure orbital elements**

Orbit leads to a Longitudinal Doppler Shift

- Estimate: consider orbit along line of slight
  - Velocity variation sum of min max velocities
- Use energy conservation

$$\frac{1}{2}v^2 - \frac{GM}{r} = -\frac{GM}{2a_2},$$

where $M = m_0 + m_1 + m_2$. Setting $r = a_2(1 - e_2)$ and $r = a_2(1 + e_2)$, we get,

$$v_{\max}^2 = \frac{GM}{a}\frac{1+e}{1-e}, \qquad v_{\min}^2 = \frac{GM}{a}\frac{1-e}{1+e}.$$

e for outer orbit!

$$2\pi P^{-1} = \sqrt{\frac{GM}{a_2^3}}$$

Way of measuring three body system directly

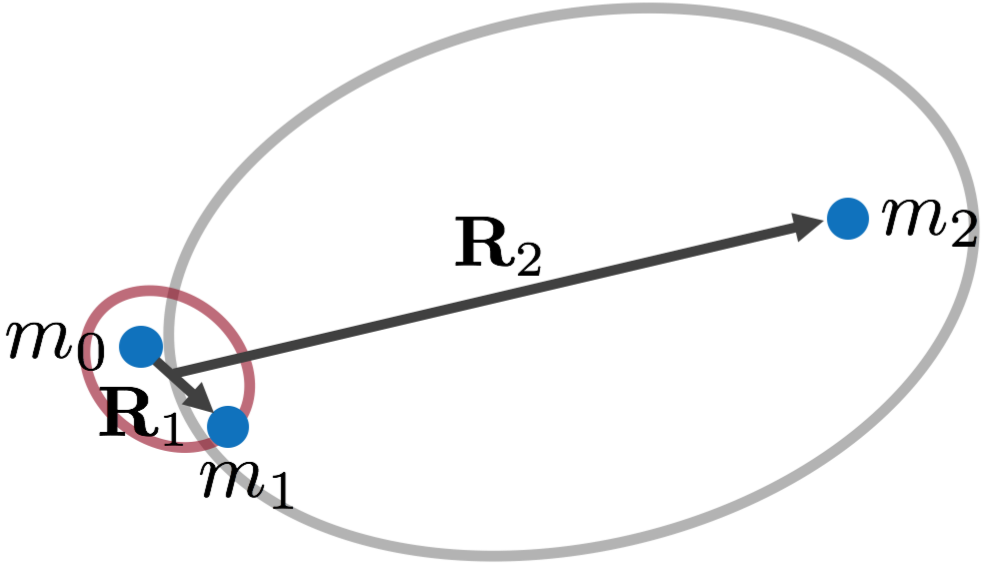

a_1 semimajor axis inner orbit
e_1 eccentricity inner orbit
$m_{1,m0}$ mass inner orbit

a_2 semimajor axis outer orbit
e_2 eccentricity outer orbit
m_2 mass outer orbit

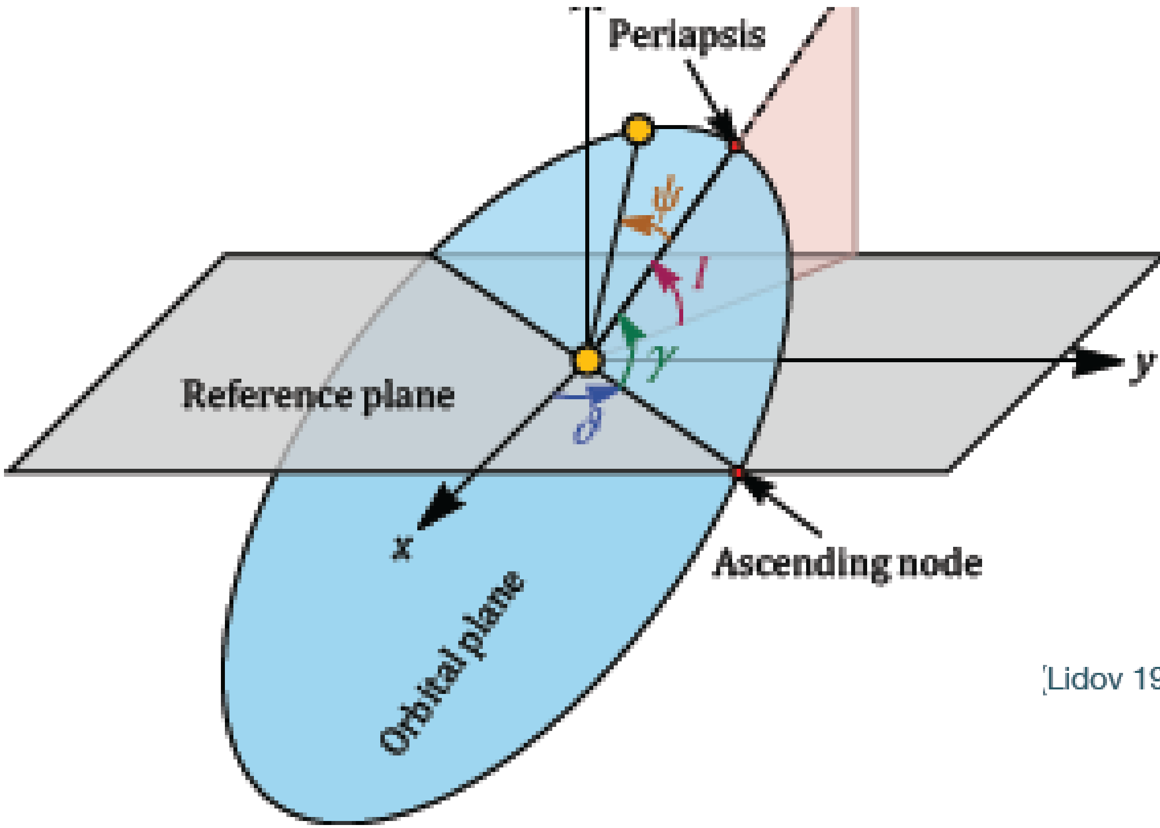

Angles to characterize both orbits
Angles to characterize relative orbital planes
KL: Average over orbits (integrate out fast modes)
Tradeoff inclination and eccentricity

(Lidov 1961, 1962; Kozai 1962; Lidov, Ziglin 1976)

barycenter motion

$$\Phi(t) = 2\pi \int_0^t f_{\rm GW}(t') \left[1 - \frac{v_{2\parallel}(t')}{c}\right] \mathrm{d}t'$$

Meiron, Kocsis, Loeb, 2016, Bonvin et al. 2017, Inayoshi et al. 2017, Robson et al. 2018

$$v_\parallel = \sqrt{GM/a_2}\cos I$$

A direct probe of density

$$2\pi P_2^{-1} = \sqrt{GM/a_2^3} \sim \sqrt{G\rho}$$

$$2\pi \cdot \mathrm{yr}^{-1} = \sqrt{\frac{G\cdot 10^6 M_\odot}{(100\,\mathrm{AU})^3}}$$

$$0.01c \simeq \sqrt{\frac{G\cdot 10^6 M_\odot}{100\mathrm{AU}}}$$

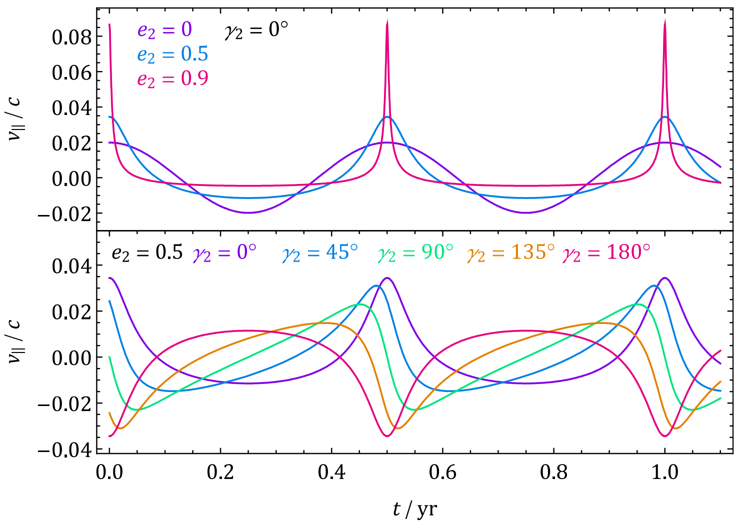

LR, ZZ Xianyu, 1805.05335

See also Robson, Cornish, Tomanini 1806.00500, Wog, Babhav, Berti 1902.01502

Observations of Interest

- Analogous to using pulsars to determine parameters of binaries
- Here can be a net phase drift reflecting time-dependent Doppler shift of outer system
  - Depends on density
    - Assuming large orbit acceleration~constant Doppler shift
- When shorter orbital period can hope to measure time-dependent Doppler shift
- Latter case (central mass, radial distance) overlaps with regime with big KL effect
  - Can observe time dependent eccentricity

Orbital motion

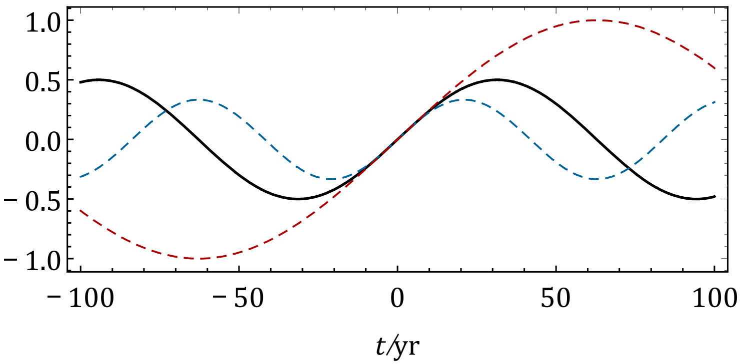

Figure 4. Illustration of the correlation between the outer orbital frequency Ω and the amplitude of the velocity u with $\Omega T_O \ll 1$. The acceleration Ωu measured during the observation time $T_O = 10$yr (gray region) from the "true" $v(t)$ (with $u_* = 0.005c$, $\Omega_* = 20\text{yr}^{-1}$) can be fitted, either by larger $\Omega = 1.5\Omega_*$ and smaller $u = u_*/1.5$ (blue dashed curve), or by smaller $\Omega = 0.5\Omega_*$ and larger $u_* = u/0.5$ (red dashed

$\Delta\Omega/\Omega$

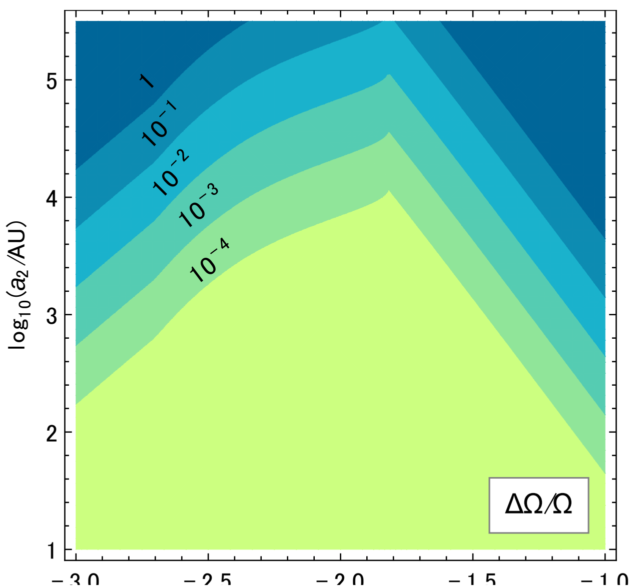

$\Delta v_{\|}/v_{\|}$

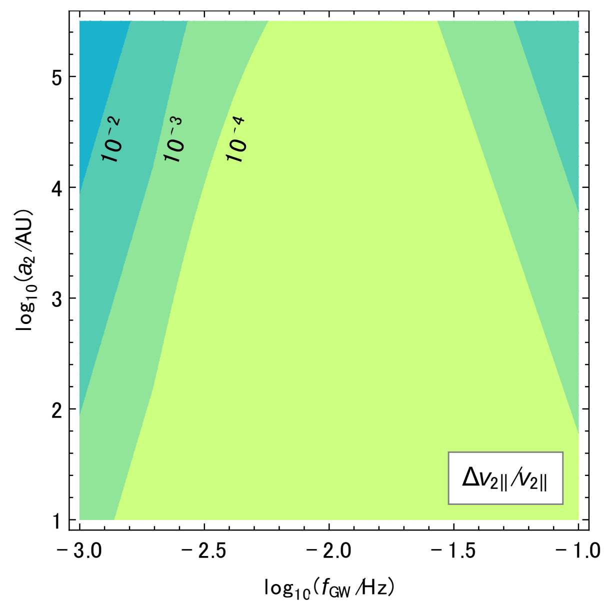

Figure 3. Fisher matrix elements $\Gamma_{\Omega\Omega}^{-1/2}/\Omega$, $\Gamma_{uu}^{-1/2}/u$, and $\Gamma_{ee}^{-1/2}/e_{1T}$, as functions of outer orbital radius a_2 and the GW frequency f_{GW}. In all plots we take a binary with $m_c = 20M_\odot$ at $r = 400$Mpc away, orbiting a third body with $m_3 = 4\times10^6 M_\odot$, observed with $T_O = 5$yr. The outer orbit is taken to be edge-on with $I_2 = 90°$. We take $e_2 = 0$ in (a,b) and $e_2 = 0.5$ in (c). Note that these quantities reduce to the relative errors of estimating the parameters Ω, u, e_{1T}, respectively, when the error correlations are weak. (cf. Fig 6).

Fisher Matrix Analysis

Can have negative chirp!

Globular Cluster events:
Can give tens of events
Different m, a: can distinguish

Also field triples precipitated by third object

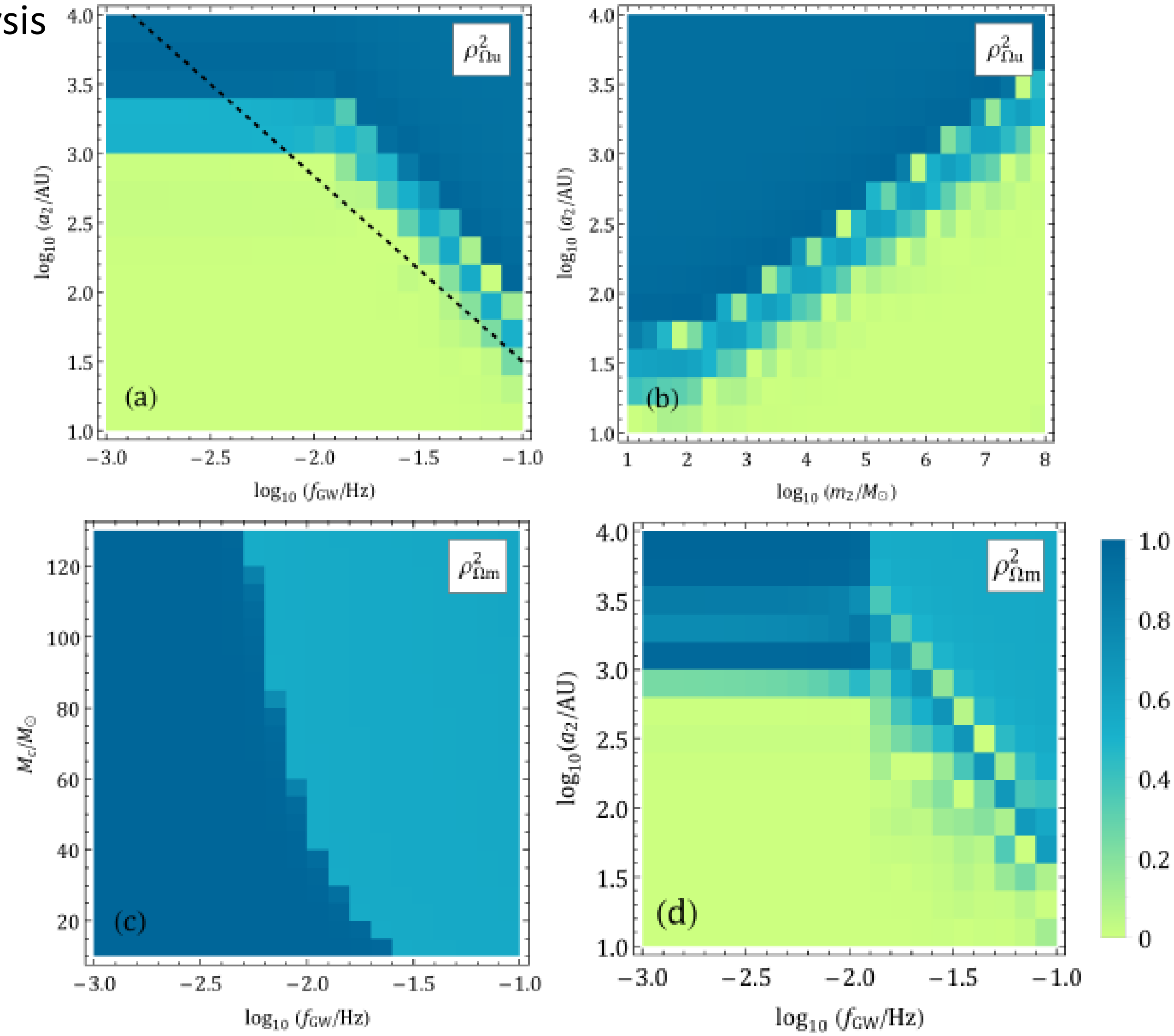

GC: Need to be close to third body but can be 10% at least

Figure 5. The error correlations $\rho^2_{\Omega u}$ (a, b) and $\rho^2_{\Omega m}$ (c, d). In (a, d), the correlations are plotted as functions of outer orbital radius a_2 and the GW frequency f_{GW} when the observation starts. In (b), $\rho^2_{\Omega u}$ is plotted as a function of a_2 and m_2. In (c), $\rho^2_{\Omega m}$ is plotted as a function of the binary's chirp mass m_c and f_{GW} with $a_2 = 10^4\,\mathrm{AU}$. We take $m_2 = 4\times10^6 M_\odot$ in (a,c,d), $m_c = 30M_\odot$ in (a,b,d), $f_{GW} = 0.01\mathrm{Hz}$ in (b). In all panels the outer orbit is taken to be edge-on with $I_2 = 90^\circ$. In (a) we show a dashed line below which there could be "negatively chirping" binaries with $\dot{f}_{GW} < 0$.

But can possibly do even better and see KL directly!

- For large a_1, eccentricity, can see binaries that enter and exit LISA window!
  - Very unique signature
  - Even one event would be amazing observation
- Frequency moves in and out of LISA window as eccentricity changes
- Peak frequency
- LISA window for 10ish solar mass BH
  - a_1~100,000 km (circular)
- With ϵ~.01 can enter LISA window for a_1~AU
- But whether we see signal very sensitive to precise eccentricity:

$$f_{\mathrm{GW}}^{m}(e_1) = \frac{\sqrt{GM_1}}{\pi}(1+e_1)^{1.1954}\frac{1}{(a_1\epsilon)^{1.5}}$$

$$\frac{\mathrm{d}e_1}{\mathrm{d}t} = \frac{5K}{J_{\gamma 1}}e_1(1-e_1^2)(1-\cos^2 I)\sin 2\gamma_1 - \frac{304}{15}\frac{G^3\mu_1 m^2}{c^5 a_1^4}\frac{e_1}{(1-e_1^2)^{5/2}}\left(1+\frac{121}{304}e_1^2\right)$$

Identifying formation channels from “final states”?Hierarchical triples

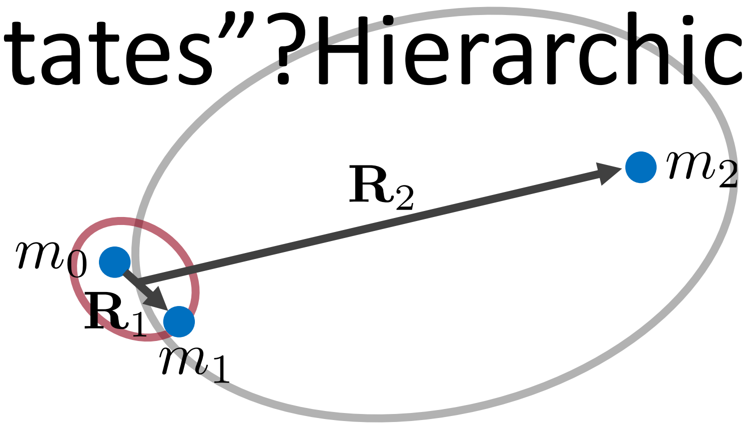

$$H = \frac{1}{2M}|\mathbf{P}|^2 + \left(\frac{1}{2\mu_1}|\mathbf{\Pi}_1|^2 - \frac{Gm\mu_1}{|\mathbf{R}_1|}\right) + \left(\frac{1}{2\mu_2}|\mathbf{\Pi}_2|^2 - \frac{GM\mu_2}{|\mathbf{R}_2|}\right) + H'$$

$$H' = \frac{Gmm_2}{|\mathbf{R}_2|} - \frac{Gm_0m_2}{|\mathbf{R}_2 + \frac{m_1}{m}\mathbf{R}_1|} - \frac{Gm_1m_2}{|\mathbf{R}_2 - \frac{m_0}{m}\mathbf{R}_1|} = \sum_{\ell=2}^{\infty} H^{(\ell)}$$

$$H^{(2)} = -\frac{Gm_0m_1m_2}{2m}\frac{R_1^2}{R_2^3}(3\cos^2\varphi - 1)$$

Averaged over orbital motions

Doubly-averaged Hamiltonian

$$H^{(2)} = -\frac{Gm_0m_1m_2}{2m}\frac{R_1^2}{R_2^3}(3\cos^2\varphi - 1)$$

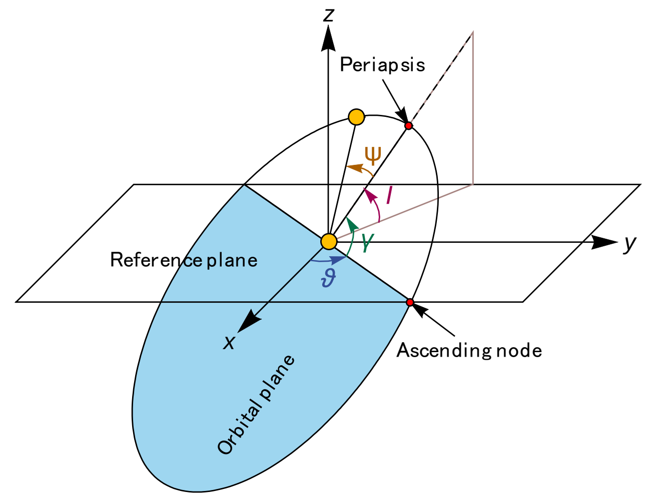

Integrate out fast modes

$$\overline{H}^{(2)} = -K(W + \frac{5}{3})$$

$$K \equiv \frac{3Gm_0m_1m_2}{8m}\frac{a_1^2}{a_2^3(1-e_2^2)^{3/2}}$$

$$W \equiv (-2+\cos^2 I)(1-e_1^2) + 5e_1^2(\cos^2 I - 1)\sin^2\gamma$$

Express in terms of orbital parameters

Conserved quantities

$$(E,\ \mathbf{J},\ E_1,\ E_2,\ J_2) \longrightarrow (a_1,\ a_2,\ e_2)$$

Constants of motion without GW

Kozai-Lidov mechanism

Lidov 1961, 1962; Kozai 1962; Lidov, Ziglin 1976

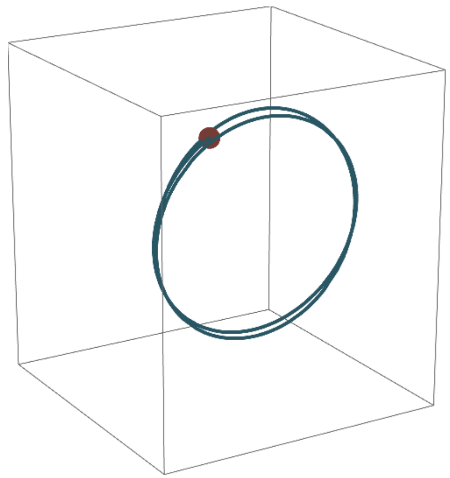

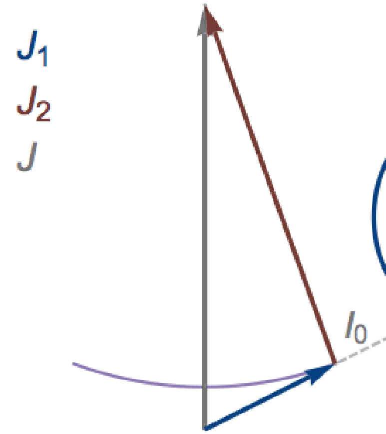

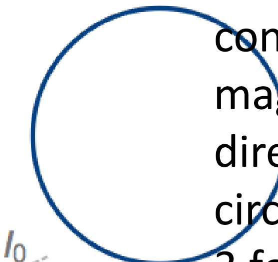

Total J conserved J2 conserved in mag not direction: circular arc
3 form triangle
J1 changes so e changes

Inner binary Shape orbit changes

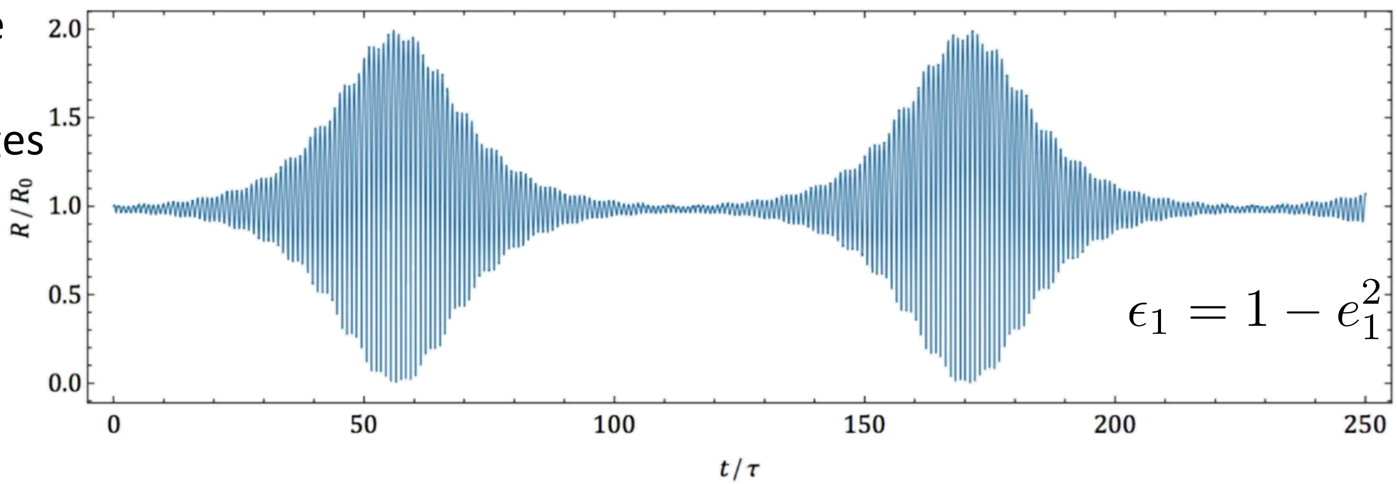

LR ZZ Xianyu 1802.05718

manifestation of KL oscillation

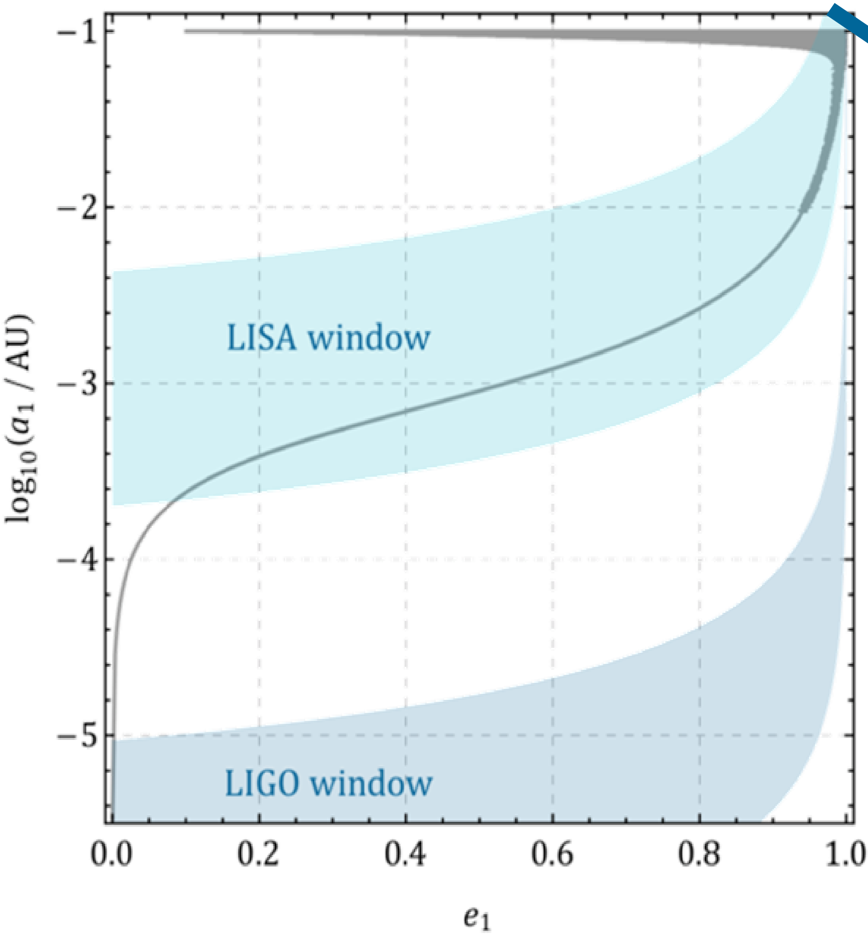

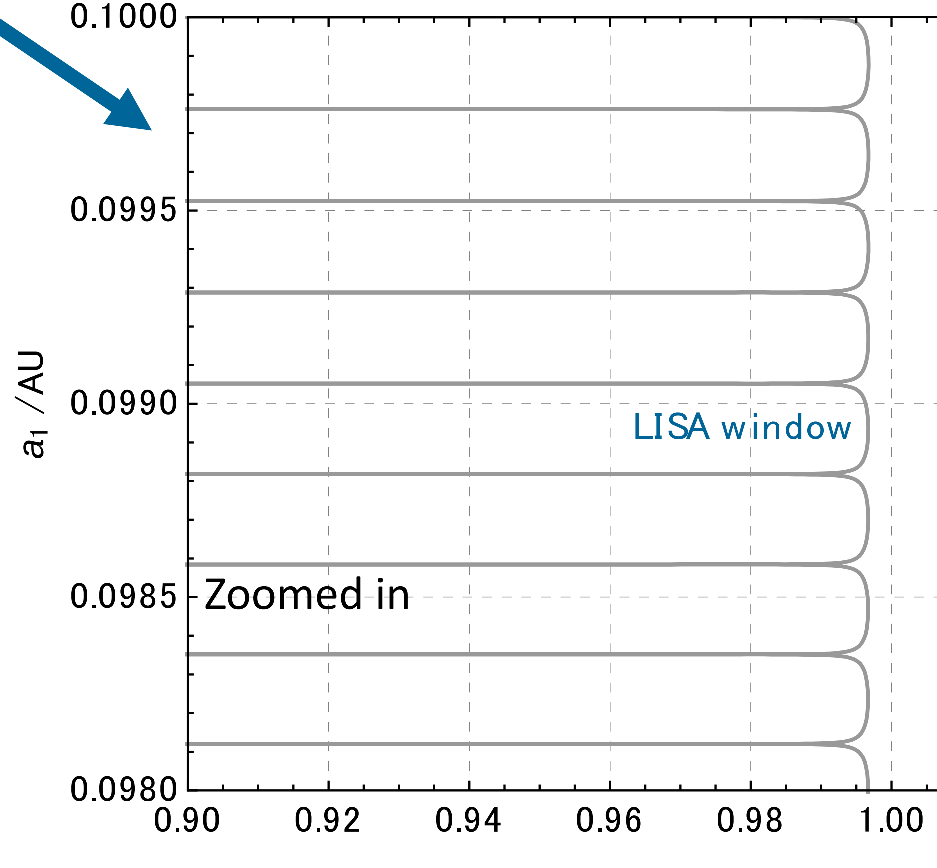

Eccentricity oscillation in LISA

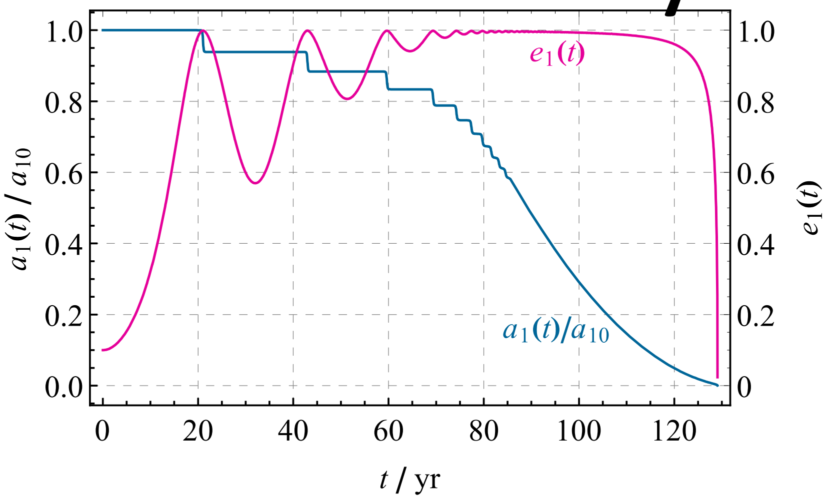

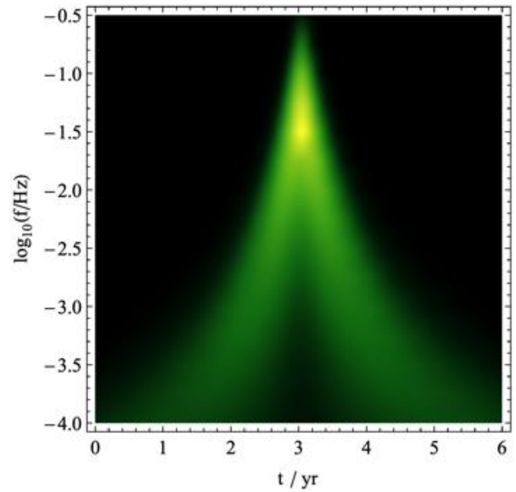

KL signal sweeps over entire LISA band

Positive and negative chirp

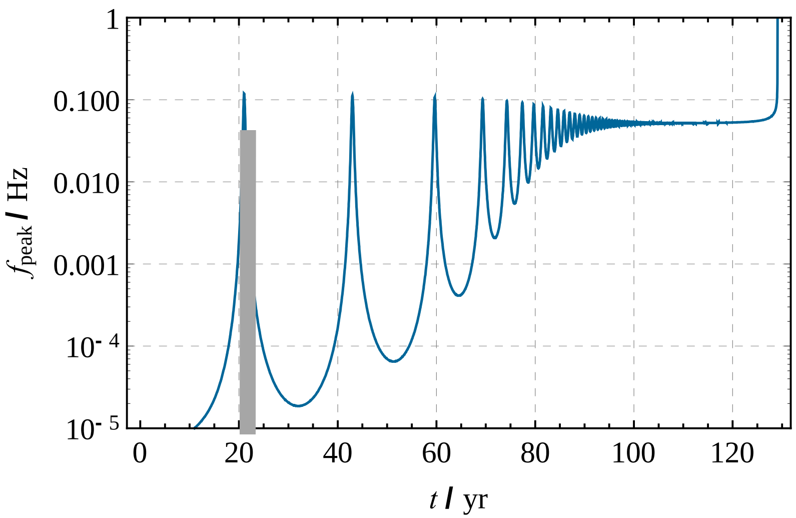

System with short merger time: can be much longer

Turns out gc or “isolated triples (Silsbee, Tremaine) can populate sweet spot in center

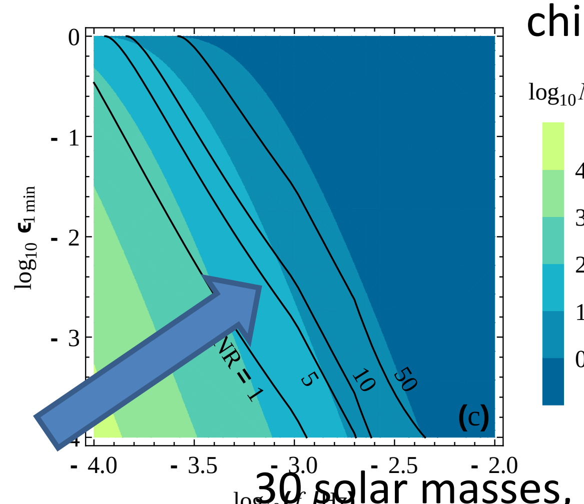

30 solar masses, 10 kpc away, our milky way

Last Topic:
Multichannel Powerful Discriminator

By Christopher Moore, [Robert Cole]() and [Christopher Berry](), formerly of the [Gravitational Wave Group]() at the [Institute of Astronomy](), University of Cambridge

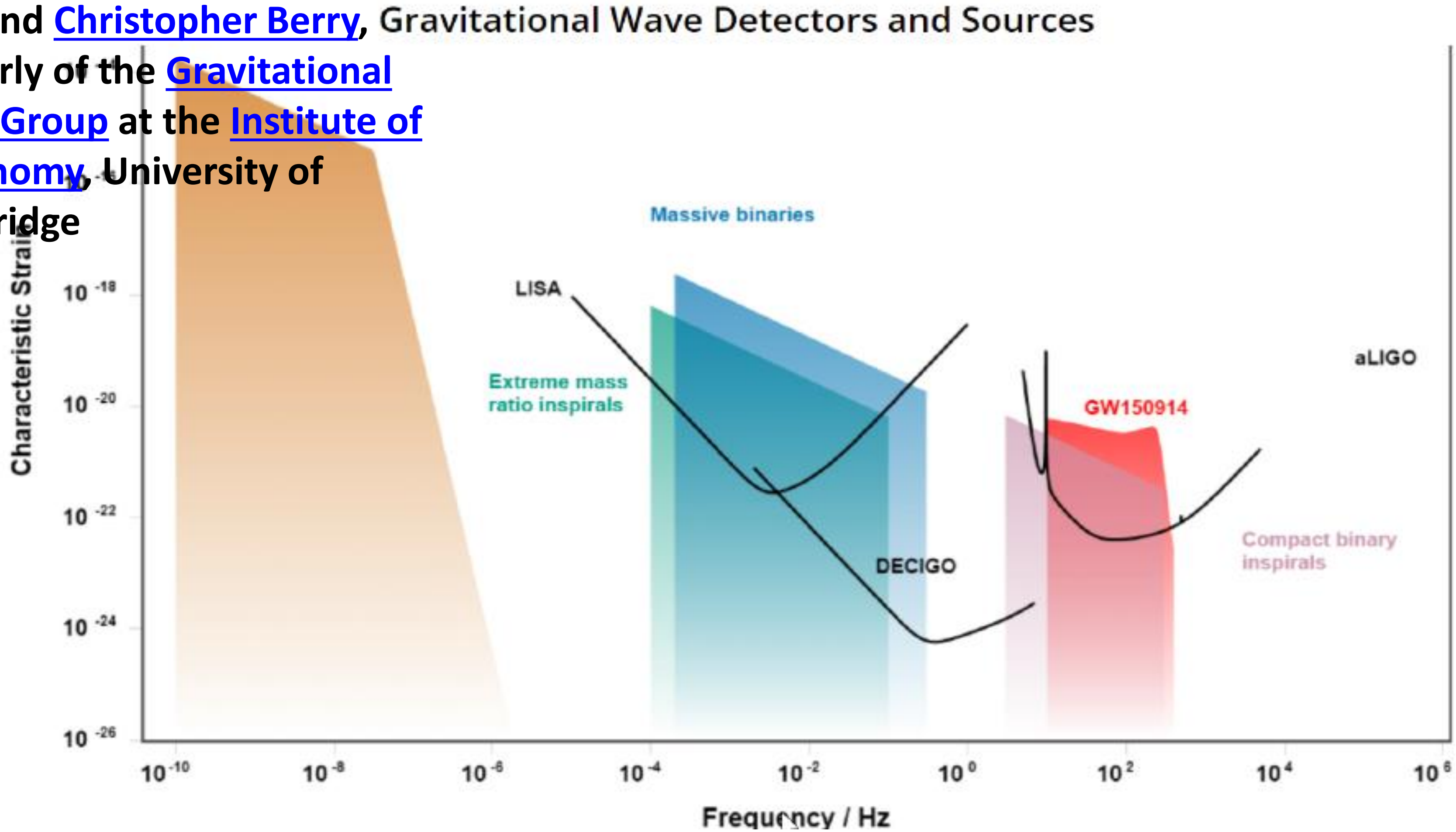

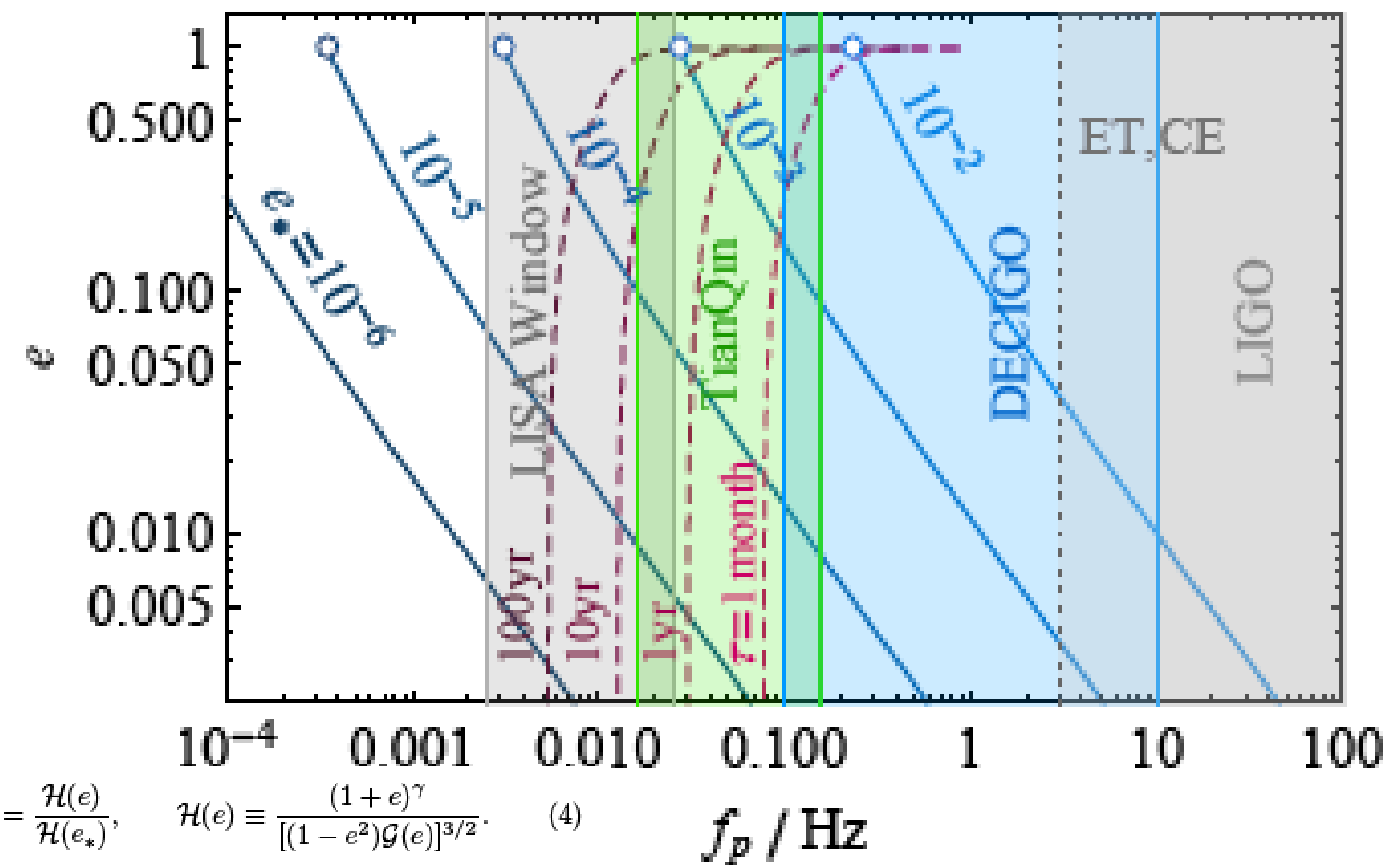

$$\frac{f_p}{f_{p*}} = \frac{\mathcal{H}(e)}{\mathcal{H}(e_*)}, \qquad \mathcal{H}(e) \equiv \frac{(1+e)^\gamma}{[(1-e^2)\mathcal{G}(e)]^{3/2}}. \qquad (4)$$

The function $\mathcal{H}(e)$ has the important property that it reaches a finite constant $\mathcal{H}(1) \simeq 1.89$ when $e \to 1$.

FIG. 1: The binary eccentricity e as a function of the peak GW frequency f_p. The five blue solid curves correspond to five reference values $e_* = 10^{-n}$ ($n = 2, 3, 4, 5, 6$) at $f_{p*} = 10$Hz, respectively. The four dashed magenta curves show the time τ to coalescence of binaries with $m_1 = m_2 = 30M_\odot$. The shaded strips show the frequency ranges covered by several GW telescopes.

$\tau \sim f^{-8/3}$

Note

- Kremer et al https://arxiv.org/abs/1811.11812 for ex simulated eccentric events LISA might see
  - They focused on what is in LISA band
  - We focus on PEAK FREQUENCY of distributions
    - Much higher than orbital frequency

$$f_p \simeq \frac{\sqrt{Gm}(1+e)^\gamma}{\pi[a(1-e^2)]^{3/2}}, \qquad \gamma = 1.1954.$$

  - Previous study of real time KL might work for nearby events
    - High e events in LISA window have long merger time since large separation
    - Radiate less power so we see only nearby events
- We are focused now on events that can make it to LIGO
  - Most don’t since peak frequency outside LISA range
    - For highly eccentric events peak frequency much bigger than orbital frequency
  - We focus here not only on what we see but also what we don’t see!

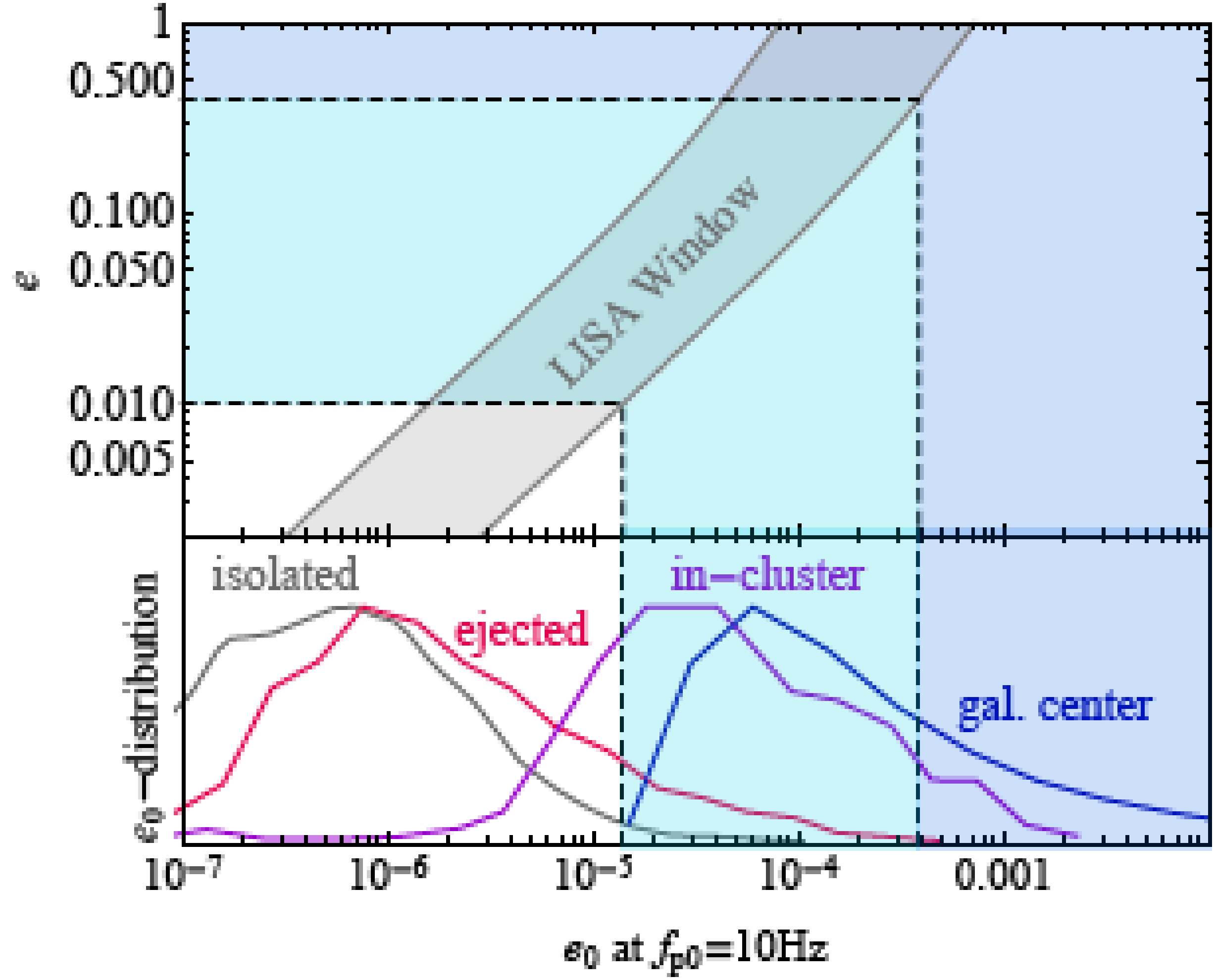

FIG. 2: UPPER: The eccentricity e in the LISA window (grey strip, same as in Fig. 1) versus the eccentricity e_* at f_{p*} =10Hz. BBHs to the lower-left of the black dashed lines could be seen in LISA if LISA is able to measure e up to 0.01 or 0.4, respectively. LOWER: Eccentricity distributions from several channels at 10Hz. The four curves corresponds to the isolated channel [3], the ejected binaries from globular clusters and the in-cluster mergers [7], and binaries from galactic centers [8]. All curves are normalized at their peak values and the overall heights do not represent relative fractions of channels.

Resolvable 'Solar' Mass Binaries in LISA as function of eccentricity

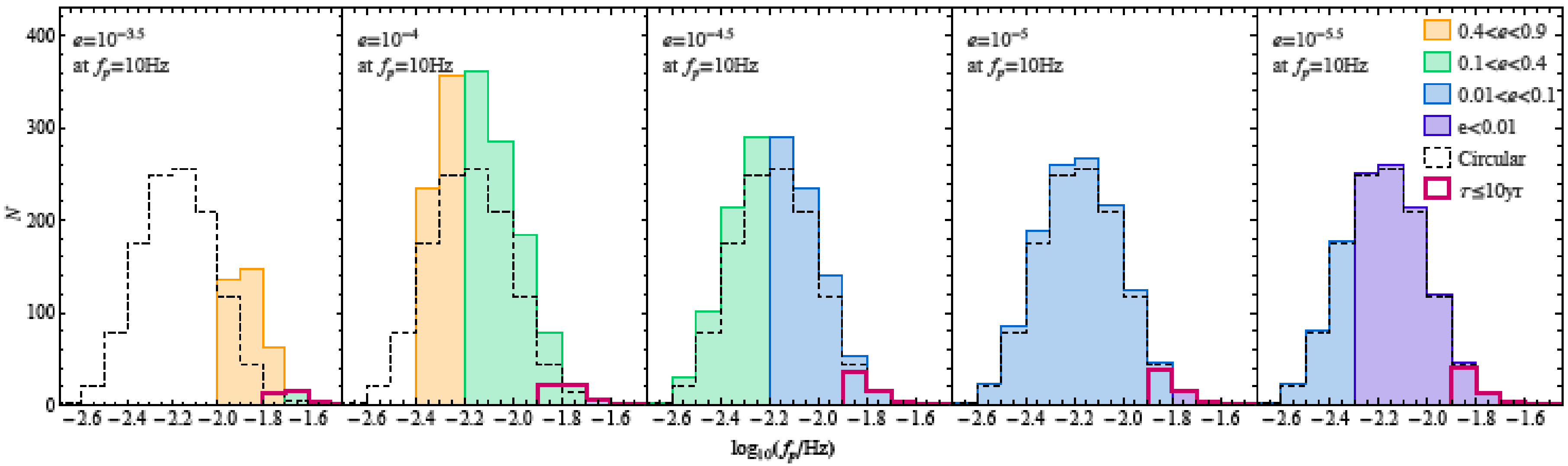

FIG. 4: The number of resolvable ($\varrho > 8$) BBHs in LISA with N2A5 configuration [11] and 10yr observation. In all panels, we use dashed black lines to show a circular distribution with $e_* = 0$, which serves as a basis to which we compare number distribution with finite e_*. In each panel, we choose a different e_* at 10Hz ranging from $10^{-3.5}$Hz to $10^{-5.5}$Hz. The purple, blue, green, and orange shadings correspond to $e_{\rm cut} = 0.01, 0.1, 0.4, 0.9$, respectively. The binaries enclosed by magenta lines merge in 10 years so are possible for joint detection with ground GW telescopes.

Eg e*=10-3 never visibly radiate
below .01 Hz

Intermediate Frequencies Can Give Powerful Discrimination

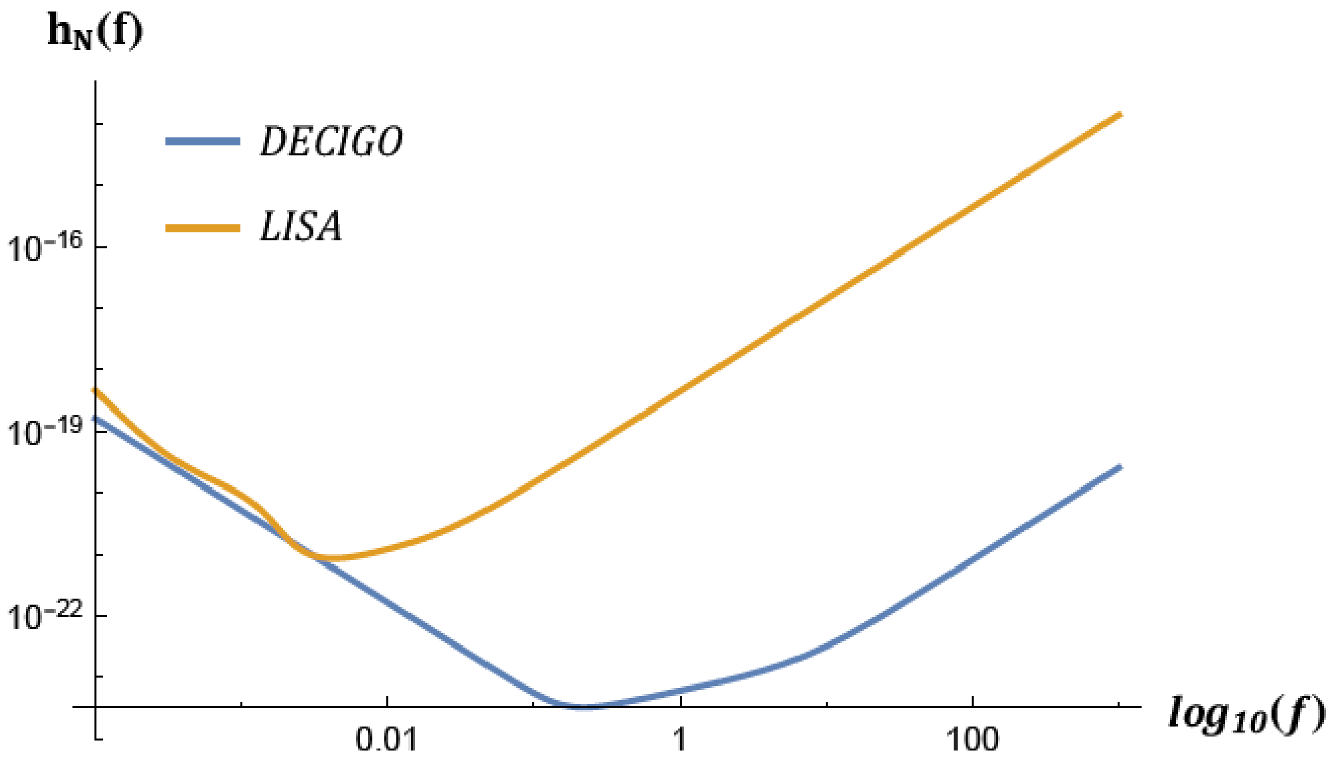

Figure 1: The noise curves of LISA and DECIGO.

Work in Progress w/Deporzio, Miccioli, Xianyu

- See how well we distinguish populations based on LISA measurements
- Again expect more events with low eccentricity for isolated events
- Higher eccentricity for dynamically generated eccentric events

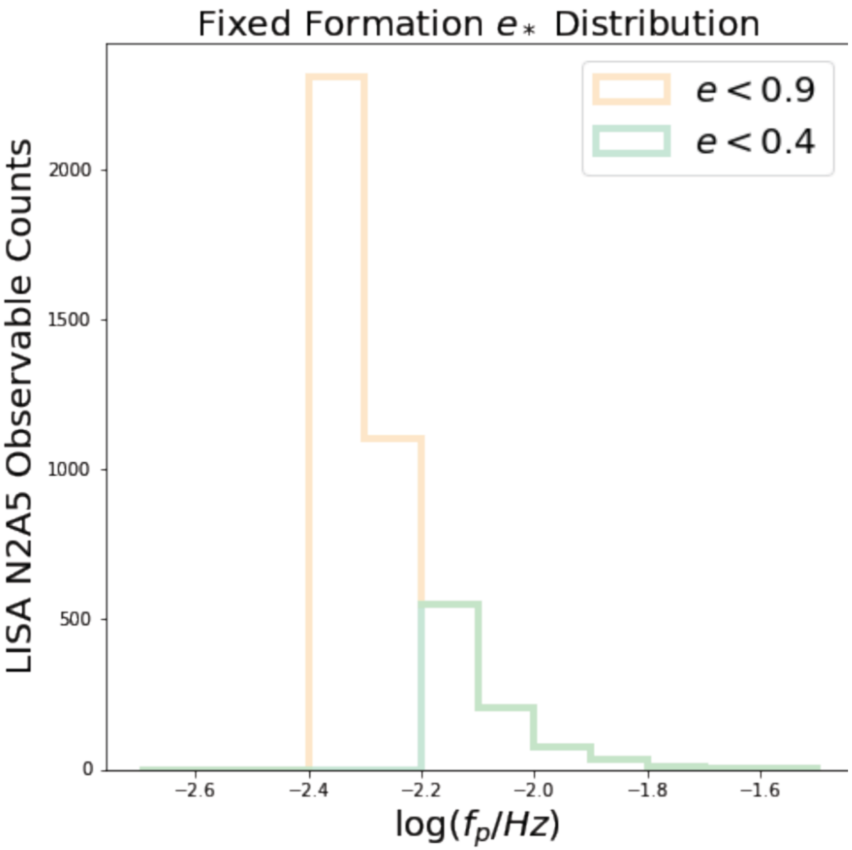

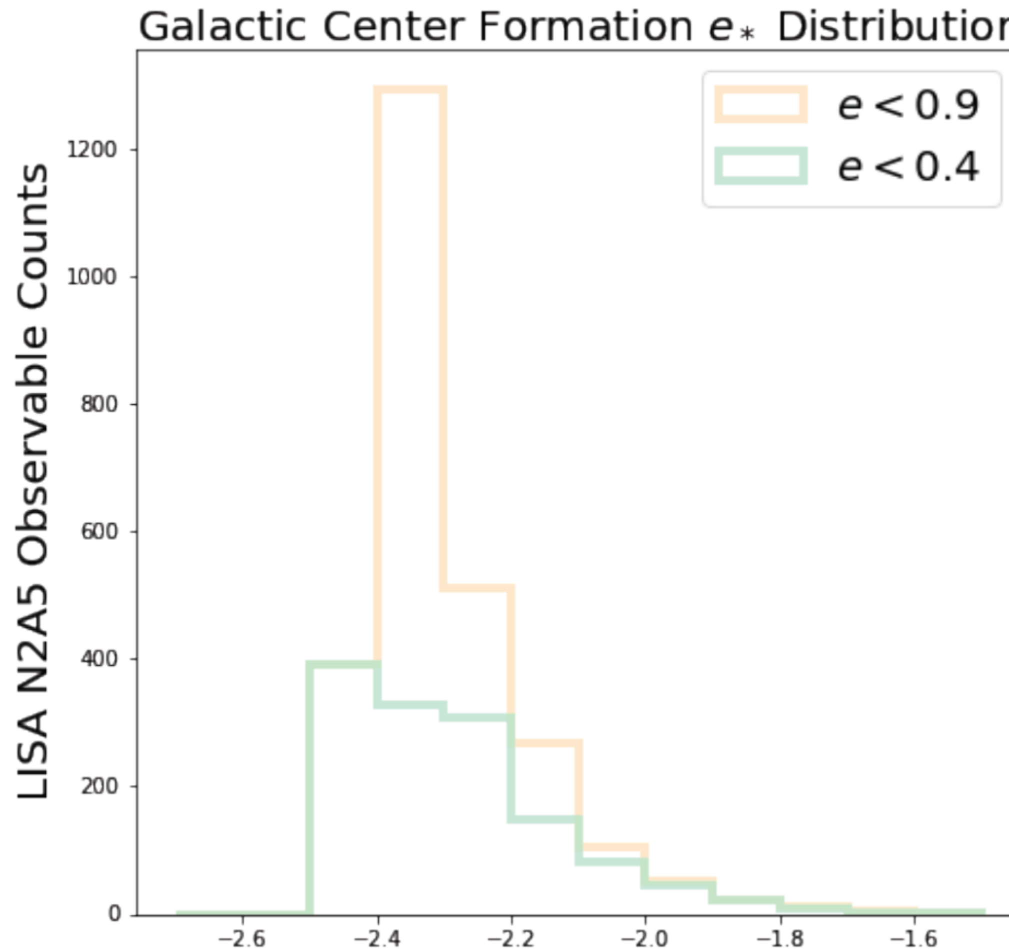

Thank you Nicholas Deporzio
for last minute plots!

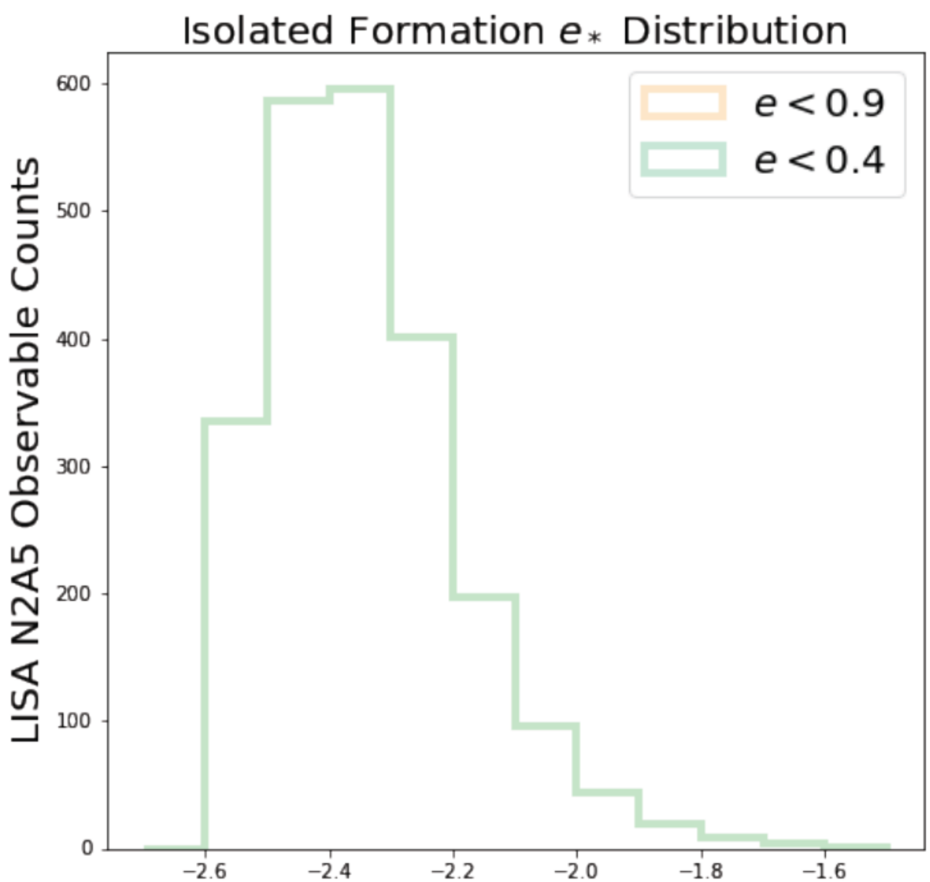
Isolated Formation e_* Distribution
LISA N2A5 Observable Counts
$e < 0.9$
$e < 0.4$
600
500
400
300
200
100
0
−2.6
−2.4
−2.2
−2.0
−1.8
−1.6

Signal to Noise w/shelest, xianyu

- Another arena where naivity paid off…
- A great deal of work has been devoted to detailed predictions of the wave forms for GW signals and building templates to accommodate them.
- However, little attention to approximations for predicting distributions and narrowing the parameter space for existing events.
  - Like pp would do
- High eccentricity means high harmonics
- Predictions computationally intensive

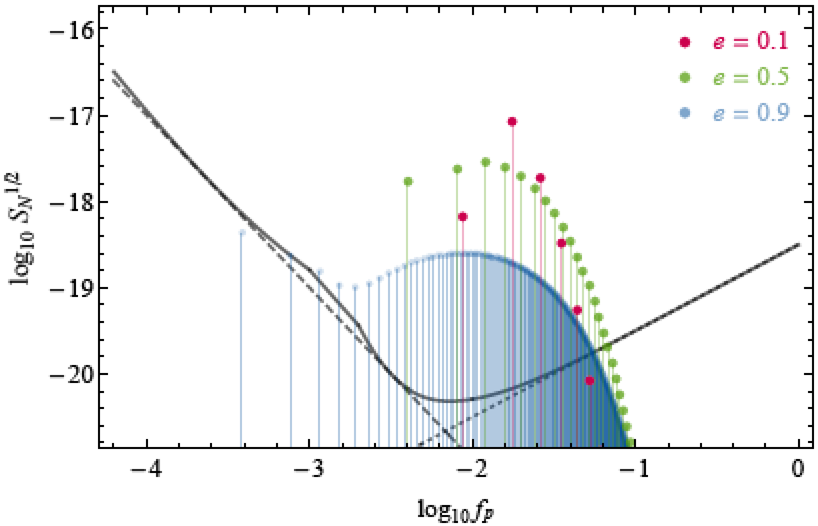

- Large spread of frequencies from higher harmonics
- We exploit approximate power law dependence of noise curves to find simple formula to approximate SNR
- Get simple analytical formula that works surprisingly well
- Essentially as first approximation use constant noise curve
    - Works well except in lower frequency regime
- Can compensate for that with simple modificaiton
- Get within a factor of two over whole range
- Will help identify theoretically useful discriminators since we can se to study populations
- Also can narrow down parameter ranges efficiently
- Also indicates larger than expected SNR for high eccentricity events

Mention other new work where pp approach helps

- RS as a way of thinking about KKLT geometry
- KKLT is a way of generating a calculable positive energy string theory vacuum
  - Compactify on CY;
    - 3-form fluxes to stabilize CS moduli
    - Branes to generate warped throat
    - gauge symmetry to destroy no-scale; nonperturbative affects stabilize Kahler moduli
  - Results in stable volume but with negative (small) energy
  - Introduce antibrane to lift energy to positive energy
  - Introduce throat to reduce positive energy from string scale

UPLIFTING RUNAWAYS

- fluxes (M, K) along the three-cycling of the deformed conifold generate a potential for the CS modulus S:
  [Douglas, Shelton, Torroba, '07, '08]

$$V_{KS} \sim \underbrace{\frac{\left|S\right|^{4/3}}{g_s(\alpha' M)^2}}_{G^{S\bar{S}}} \left| \underbrace{\frac{M}{2\pi i}\log\frac{\Lambda_0^3}{S} + i\frac{K}{g_s}}_{D_S W} \right|^2$$

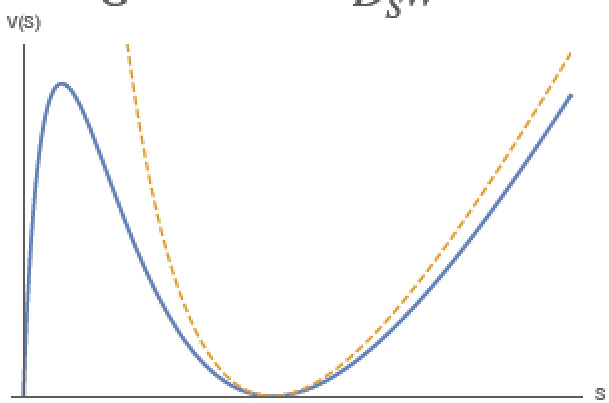

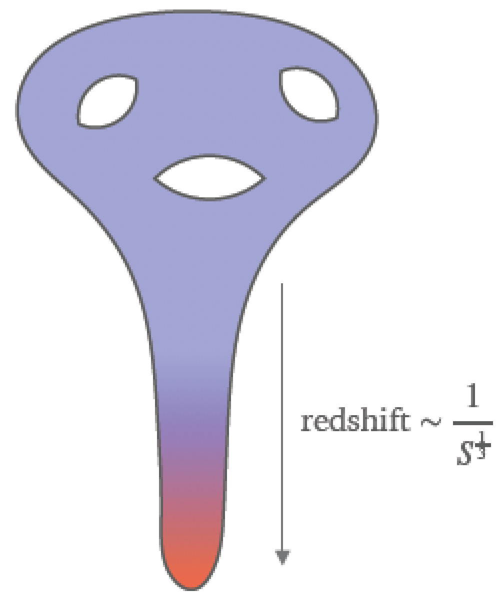

UPLIFTING RUNAWAYS

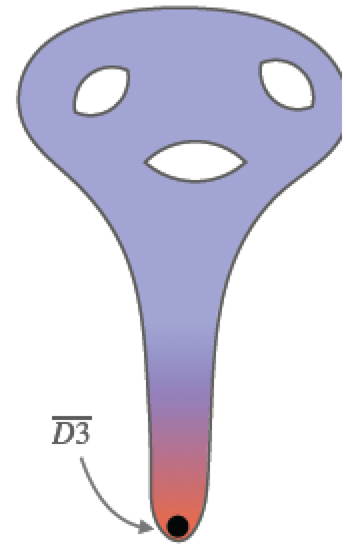

- addition of an anti-brane:
  contributes to the potential:

$$V_{\overline{D3}} \sim 2e^{4A}T_{D3} \sim \frac{\left|S\right|^{4/3}}{g_s(\alpha' M)^2}$$

- combined potential:

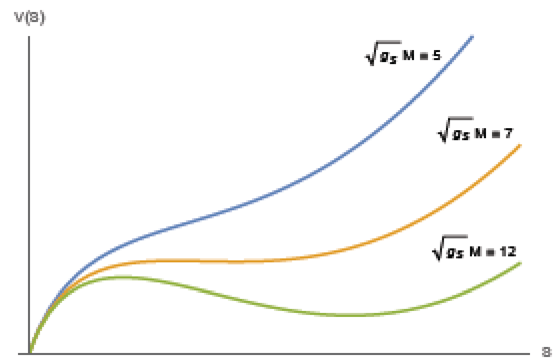

- runaway to infinite throat ($S \to \infty$ = KT-solution) unless:

$$g_s M^2 > \gamma_{\overline{D3}}^2 N_{\overline{D3}}\,, \qquad \gamma_{\overline{D3}} \approx 6.8$$

When adding antibrane need off-shell potential

Originally identified in **
Easy to see in 5d EFT (LR)

Anti-brane instability:
Requires knowledge of the (off-shell) potential away from the minimum!

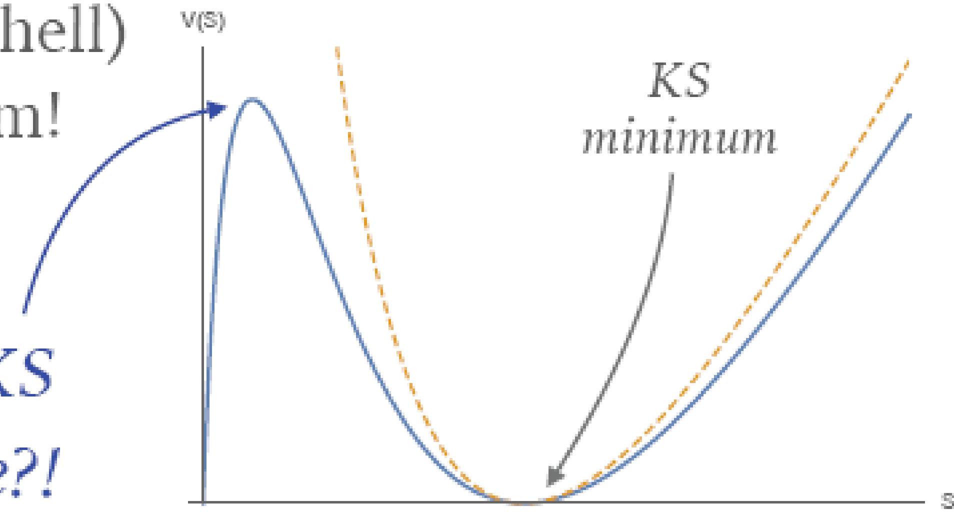

However, instability

- Many debates about EFT
- Bena, Dudas, Grana, Lust identified a straightforward instability
- Even easier to see in 5d picture (LR)
- Add potentials and find runaway direction for "radion"
  - Radion was the conifold deformation parameter
  - Sets size of warped throat

EFT Puzzles

  - Radion was the conifold deformation parameter
  - Sets size of warped throat
- Would SUSY ever break?
  - Gravitino condensate
- Is there really a nonperturbative nearby minimum?
  - This was our first track to find what is missing
  - Turns out susy constraints such that runaway not resolved

Current work

- Turns out EFT for S field was not complete
  - Need to take off shell
- Account for gauge constraints of vanishing off diagonal metric components
  - In presence of warp factor
- From EFT perspective turns out theory was not complete EFT
  - Light modes emitted
  - Kahler moduli are stabilized
  - But KK modes in warped throat are not

From Luest slides

COMPLEX STRUCTURE OF THE DEFORMED CONIFOLD

- First: understand gauge fixing without warping:

$$ds^2_{10} = ds^2_4 + ds^2_{DC}$$

- Gauge fixing of Calabi-Yau deformations:

$$g_{ij} \to g_{ij} + \delta g_{ij}$$

$$\Rightarrow \qquad g^{ij}\delta g_{ij} = 0 \qquad \qquad \nabla^i \delta g_{ij} = 0$$

(traceless) *(harmonic)*

(will get modified in the presence of warping!)

- Deformed conifold:

$$\delta g_{ij} = \partial_S g_{ij} \sim \frac{1}{S} g_{ij}$$

harmonic but not traceless!

COMPLEX STRUCTURE OF THE DEFORMED CONIFOLD

- Add compensating diffeomorphism:

$$\delta g_{ij} = \partial_S g_{ij} + 2\,\nabla_{(i}\eta_{j)}$$

Ansatz:

$$\eta = \left(\eta^\tau(\tau),0,0,0,0,0\right)$$

Solution:

$$\eta^\tau(\tau) = -\frac{1}{2S}\frac{\sinh(2\tau)-2\tau}{\sinh^2\tau}$$

- Interpretation:

Replace τ with "new" S-dependent radial variable: $\tau \to T(\tau, S)$

$$\frac{dT}{dS} = \eta^\tau\left(T(\tau,S),S\right) \longrightarrow$$

Analytic solution:

$$T(\tau,S) = F\left[F^{-1}(\tau) - \tfrac{1}{4}\log\tfrac{S}{S_0}\right]$$

with $F(x) = \frac{1}{2}\log\left[\sinh(2x) - 2x\right]$

- The radial coordinate as a function of S:

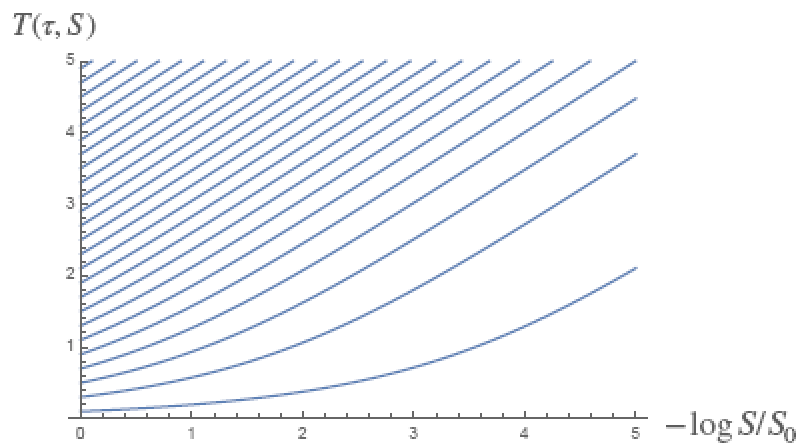

- UV behavior ($\tau \to \infty$): $T(\tau,S) \to \tau - \log S/S_0$

A POTENTIAL FOR THE WARPED DEFORMED CONIFOLD

- Numerical evaluation of the constraint yields the following warp factor:

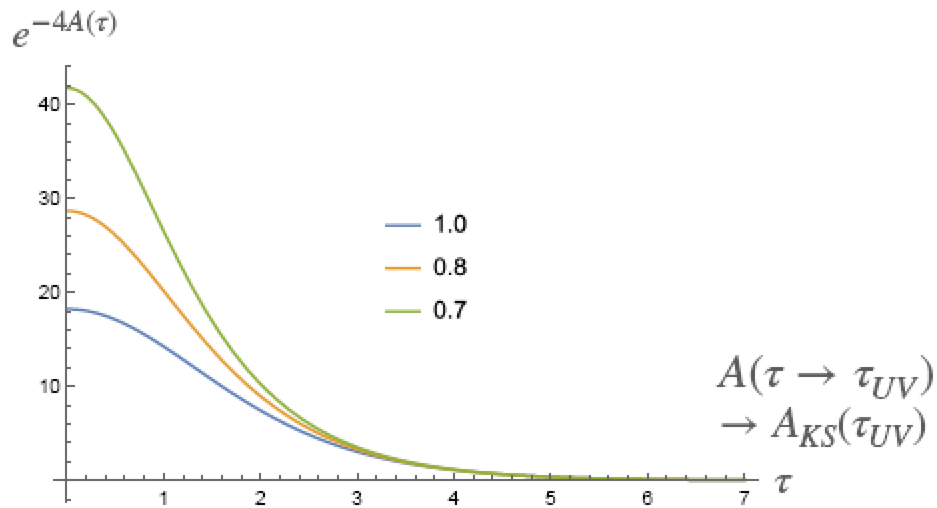

- In the IR:

$$e^{-4A(\tau=0)} \sim \frac{1}{S}$$

(on-shell) KS warp factor:

$$e^{-4A(\tau=0)} \sim \frac{1}{S^{4/3}}$$

A POTENTIAL FOR THE WARPED DEFORMED CONIFOLD

- Resulting potential:

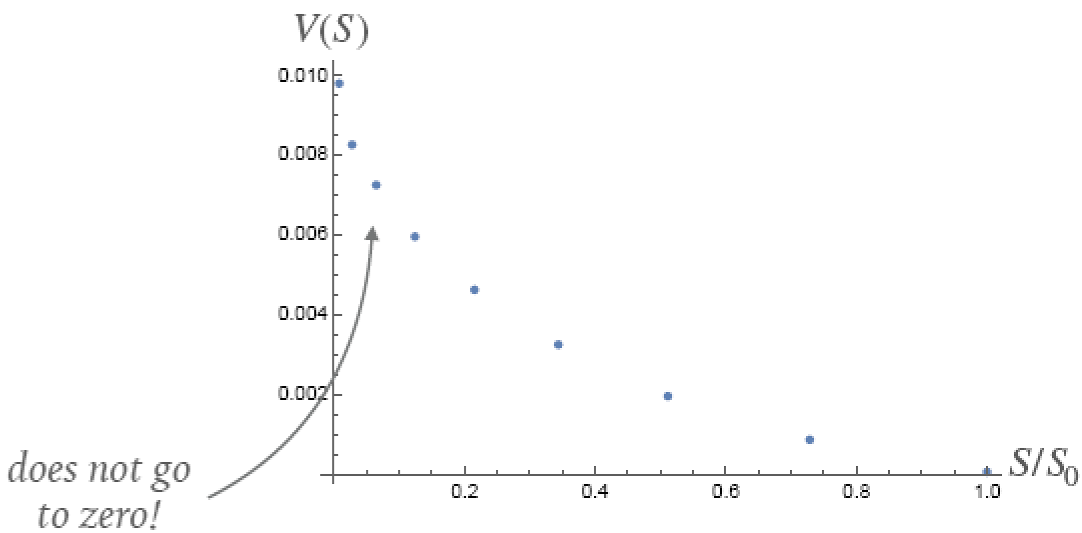

$\rightarrow$ no antibrane instability!

EFT and resulting potential was wrong
Need to account for changing compactification volume—more than fixed warp factor

Another application of PP models

- Karch-Randall braneworld
- Apparently innocuous extension of RS braneworld
- Brane has negative cc/aka AdS brane
- Interesting features
  - Even with UV brane includes half the boundary
  - Double holography
  - Had a massive graviton! No exactly zero mode
    - Yet still communicates “4d” gravity

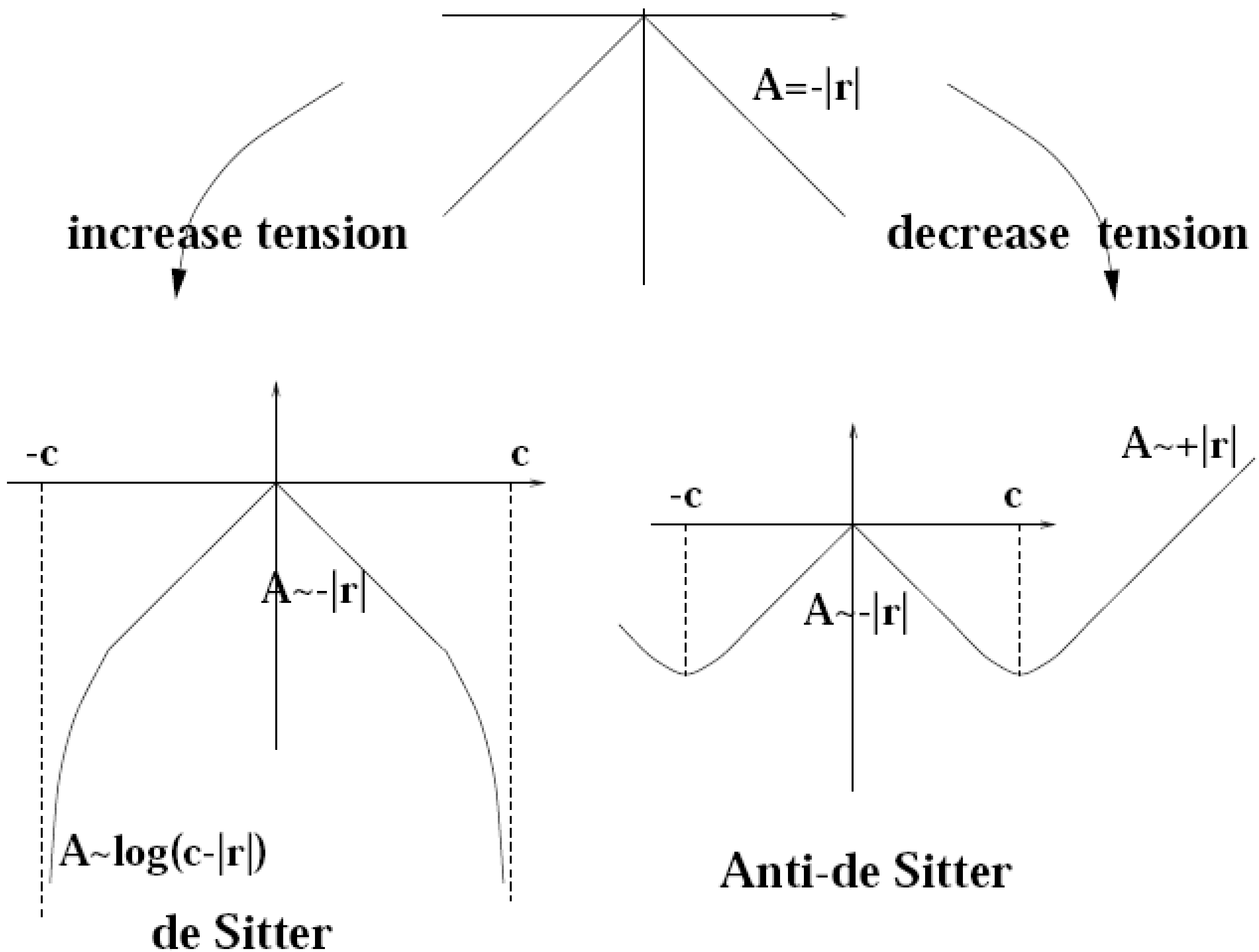

Figure 1: The behavior of the warp-factor for $\Lambda = -1$, 0 and 1.

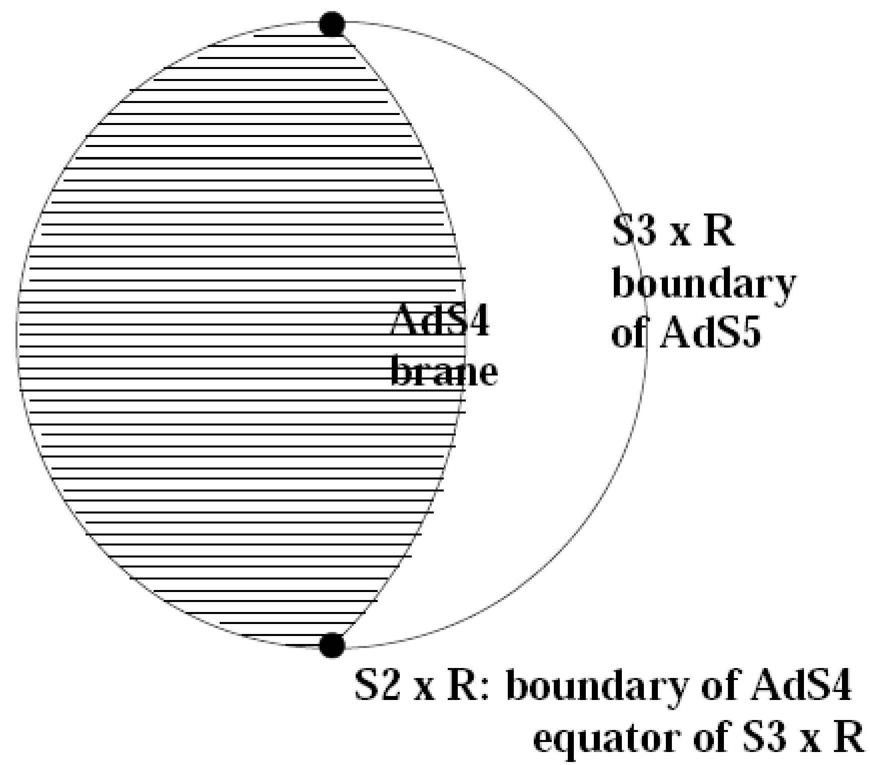
S3 x R
boundary
of AdS5
AdS4
brane
S2 x R: boundary of AdS4
equator of S3 x R

Useful for Information Transfer/Entanglement Entropy Calculations

- Was independently observed
- Such models provide way to couple brane and bath (on boundary)
- Allows for "evaporation" and because of double holography allows for calculation
- Our group (G7) Geng, Karch, Perez-Pardavilac , Suvrat Raju, LR, Riojas, Shashi used it as a tool to study
  - Role of long-range gravity: one vs two branes
  - Role of mass in allowing consistency with a Gauss Law constraint
- Upshot is both matter!

Conclude

- We are so far advanced that further advances elusive
- Doesn’t mean we know all the answers. Not nearly.
- But need clever insights, new domains to search
- Lots of interesting work on axions
- And light particles
  - Might or might not be there but still room to explore
- Gravity waves we are just beginning to think about in context of BSM (but challenging)
- And pp methods and models have a role in deeply theoretical issues as well
- Astro Dark will be a rich arena for years to come

Conclusions

- New era of gravitational wave astronomy
- Potential for new types of measurements to do BSM physics
- But also potential for Beyond Standard Astronomy (BSA)
- Hope to determine origin of “stellar mass” Black Hole Binaries
  - Finite eccentricity, Barycenter motion, Eccentricity oscillations
- But Multichannel can be most powerful discriminator
- LISA NOT seeing events
  - And an intermediate frequency observatory that does see them
- Real hope of learning more